Modeling the Active Center of Proteins that Contain Iron in a Mixed Nitrogen/Oxygen/Sulfur Coordination Environment

by

Dipl.-Chem. Dirk Schweitzer

Precandidacy Exam
"In-Field"
Department of Chemistry
University of Washington
Seattle, Washington, U.S.A.

Spring Quarter 1998

Abstract:

In this paper a "progress report" of studies on model compounds of nitrile hydratase is presented. Nitrile hydratase, which catalyzes the hydration of nitriles to amides, contains a low-spin non-heme Fe(III) in its active center. The iron in the active form of the enzyme is coordinated by five protein based ligands and one water molecule. The exact identity of the protein based ligands remains obscure. It has been proposed in the literature that histidine imidazole nitrogen, amide nitrogen, cysteine sulfur, and/or cysteine-sulfinic acid oxygen is coordinated to the metal center. Studies on nitrile hydratase indicate that its activity is regulated by binding NO (nitric oxide, nitrogen monoxide). The uncertainty of the coordination environment of the active site iron, the unusual spin state of the active site iron, and the novel mechanism of activity regulation provide numerous questions. The aim of the research summarized in this paper is to provide an answer to some of these questions. The research described in this paper provides one with the prospect of understanding the principles in the relationship between structure and function of a variety of biologically relevant metalloenzymes, including nitrile hydratase, desulfoferrodoxin, neelaredoxin, and, most likely, other not yet discovered metalloenzymes.

Table of Contents:

1.) Introduction page 3

2.) Nitrile Hydratase page 4

3.) Proposed Mechanism of Hydration of Nitriles to form Amides by Nitrile Hydratase page 16

4.) Challenges of Modeling Low-spin Fe(III) in a N/S Coordination Environment page 18

5.) A Model of the Active Center of the Intermediate Form of Nitrile Hydratase page 18

6.) A Model of the Active Center of the NO-Inactivated Form of Nitrile Hydratase page 22

7.) Electronic Structure of Model Compounds page 32

8.) Experimental Section page 38

9.) Further Work page 50

10.) Conclusions page 56

11.) References page 57

1.) Introduction:

Bioinorganic chemistry is a discipline of chemistry that investigates the functions and roles of 'non-organic' elements within biological systems. This discipline emerged in the 1960's. The rapid development of analytical methods enabled scientists to recognize that metal ions play significant roles in biological systems. For example, it was found that a majority of all proteins require one or more metal ions to exercise their biological activity. Consequently, an important aspect of bioinor-

ganic chemistry involves the study of how a metal ion influences the biological activity of an enzyme. The research described in here attempts to contribute to an understanding of some aspects of this question.

One of the metals most commonly present in active centers is iron. Iron can occur in an active center as a heme unit (*e.g.* cytochrome P450), as a diiron-carboxylate unit (*e.g.* hemerythrin), as an iron-sulfur cluster (*e.g.* ferredoxins and nitrogenase), or as a mononuclear iron center.[1] Only a few number of mononuclear iron centers are known to contain iron in a mixed nitrogen/oxygen/sulfur coordination environment. They include nitrile hydratase, center II of desulfoferrodoxin[2], and possibly, neelaredoxin[3].

Center II of desulfoferrodoxin was shown to be an octahedral $FeN_4S_1X_1$ site, with the cysteine being opposite of the open coordination site. The symbol X is used to denote an open coordination site, which might be occupied by a rapidly exchanging water molecule. Based upon protein occurrence, sequence similarity, UV/vis data, and EPR measurements, it was proposed that the active center of neelaredoxin exhibits structural similarities to center II of desulfoferrodoxin. The iron centers in desulfoferrodoxin and neelaredoxin are always high-spin. So far, the functions of desulfoferrodoxin and neelaredoxin are unknown. However, it is likely that they are involved in electron transfer.

2.) Nitrile Hydratase:

Nitrile hydratase (NHase) is known to occur either as an iron or as a cobalt-containing enzyme. Organisms that are known to express the Co-containing enzyme are *Rhodococcus rhodochrous* J1[6], *Pseudomonas putida* NRRL-18668[15b], and *Agrobacterium tumefaciens*[19]. An organism

can express both the Co-containing enzyme and the Fe-containing enzyme simultaneously.[19] The investigated Co-containing NHases have a higher activity and a higher stability than the investigated Fe-containing NHases. In spite of this, the discussion in this paper will be concentrated upon Fe-containing nitrile hydratases.

2.1.) Nitrile Hydratase - Its Physiological Role and Its Application:

An iron-containing Nitrile hydratase has been isolated from a number of bacterial species. They include *Rhodococcus sp*. N-771, *Rhodococcus sp*. R312 (= *Brevibacterium* R312), *Comamonas testosteroni* NI1, and *Pseudomonas chlororaphis* B23. The physiological role of NHase is to catalyze the hydration of nitriles to the corresponding amides as shown in figure 1. This might be necessary to remove toxic nitriles[23], to use nitriles as a source of carbon and nitrogen[24], or to synthesize plant hormones[19]. The production of plant hormones by bacteria seems to be essential for a symbiosis between bacteria and plants. Most NHases exhibit a great substrate variability.

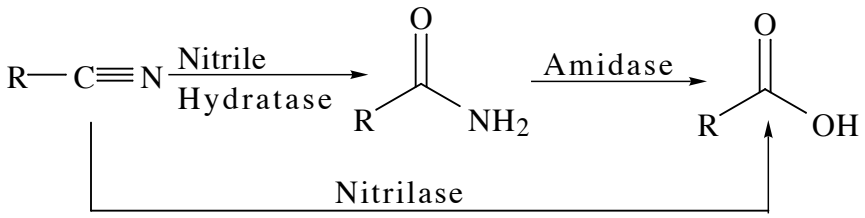


Figure 1. Biological Pathways to Convert Nitriles to Carboxylic Acids.

Related chemical transformations are catalyzed by nitrilase[10] and amidase[11]. Nitrilase converts nitriles to their corresponding acids and ammonia. Amidase converts amides into their corresponding acids. *Rhodococcus rhodochrous* J1 contains the gene for both NHase and

nitrilase. However, only one of the two proteins is expressed depending upon the substrate present when the bacterium is cultivated. Whether or not *Rhodococcus rhodochrous* J1 contains a gene for amidase is unknown to the author of this paper. It has been shown that *Agrobacterium* and *Rhizobium* bacteria express both NHase and amidase simultaneously.[19] Whether or not *Agrobacterium* and *Rhizobium* bacteria contain a gene for nitrilase is unknown to the author of this paper.

NHase has found a variety of applications. Immobilized *Rhodococcus rhodochrous* J1 cells, which contain nitrile hydratase, are used in a 30,000 t/y production process to hydrate acrylonitrile to acrylamide.[8] NHase was shown to be effective in the removal of nitriles from waste.[9] Further, NHase has the potential to be employed in many industrial and laboratory scale chemical processes because the reaction occurs under very mild conditions.[25] Also, NHase can be used in the enantioselective synthesis of amides.[15b,c,d]

2.2.) Nitrile Hydratase - Studies of the Enzyme:

Studies on NHase from *Rhodococcus* N-771 indicate that NHase is an αβ heterodimer, with the α and β subunit each having approximately a molecular weight of 27.5 and 28 kDa, respectively.[28] In NHase from *Rhodococcus* N-774 the α subunit is comprised of 207 amino acids and the β subunit is comprised of 212 amino acids.[16] The iron containing center is located on the α subunit.[14] Sequence alignment indicates that the α subunit of NHase contains a conserved sequence: -Cys-Thr/Ser-Leu-Cys-Ser-Cys-Tyr/Thr-.[15] This sequence is conserved in both iron and cobalt containing NHases. In the crystal structure of NHase from *Rhodococcus* sp. R312 one iron ion was located in the active center.[16]

NHase contains in its active center either a low-spin Fe(III)[17] or a low-spin Co(III)[15b]. To date, NHase is the only non-heme enzyme known to contain a low-spin Fe(III). It is remarkable that NHase, which catalyzes a reaction in which water attacks a substrate, contains Fe(III) or Co(III) in its active center instead of Zn(II) as most hydrolytic enzymes do.[18] A possible explanation for this might be that Fe and Co are the only readily biologically accessible metals that can form a +3 ion. If one assumes that the nitrile substrate must be polarized, as it is in the proposed mechanism in chapter 3, prior to nucleophilic attack upon the nitrile carbon then it is understandable that an ion with a +3 charge is required for NHase to exercise its catalytic function. A metal ion with a +3 charge is a much stronger Lewis acid than a metal ion with a +2 charge. It would be interesting to measure the activity of NHase when the Fe(III) or Co(III) ion is replaced by other metal ions, including divalent ones. To the best of the author's knowledge no such experiment has been reported.

An immense number of articles have been published in which studies of the active center of NHase were reported. Among the techniques that were used to gain information about the active center of NHase are UV/vis, FTIR, EPR, EXAFS, ENDOR, resonance Raman, Mössbauer, mass spectrometry, x-ray crystallography, and light irradiation. However, no mutagenesis studies were performed. This is surprising since mutagenesis studies could have answered the question if certain amino acids (*e.g.* cysteine and histidine) are in fact necessary for NHase to exercise its catalytic function. Prior to conducting the x-ray crystallographic analysis, mutagenesis studies could have helped significantly in assigning an active site structure to the measured spectroscopic data.

All reports, except one, on the structure of the active center of NHase seem to agree upon that the iron is in a mixed histidine-cysteine coordination environment containing two cysteine-sulfurs, three histidine-imidazole-nitrogens, and an open coordination site, which is occupied by a rapidly exchanging water molecule. In contrast to this, the x-ray structure of NHase shows that the iron is coordinated by three cysteine-sulfurs and two amide-nitrogens.[16]

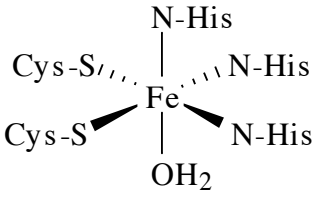


Figure 2. Schematic Representation of the Structure of the Active Site of NHase as Determined by Spectroscopic Methods.

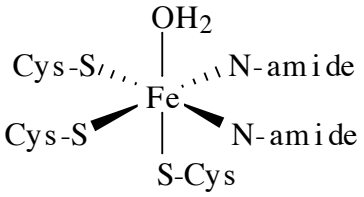


Figure 3. Schematic Representation of the Structure of the Active Site of NHase as Determined by a X-ray Crystallographic Study.

There are two possible explanations for the discrepancy between the spectroscopic and the x-ray crystallographic results. Firstly, there could have been a cardinal error in solving the crystal structure. Such an error could be a wrongly traced chain. This is highly unlikely considering that the x-ray structure placed the active center within the conserved sequence, *vide supra*. Secondly, this discrepancy might result from the fact that in the interpretation of the spectroscopic data it was never considered that an amide-N could be coordinated to the iron center. Such a coordination mode was unexpected by the researchers. However, if the researcher would have done mutagenesis studies they would have realized, most likely, that the histidines are not necessary for catalytic activity. Now researchers should reinterpret their spectroscopic data, since from the current situation it must be concluded that it is

inherently impossible to distinguish between an amide-N and a histidine-imidazole-N by EPR, EXAFS, ENDOR, and resonance Raman techniques. Maybe it will be possible to establish criteria that will enable the distinction between amide-N and imidazole-N in the future.

When Fe-containing NHases were studied it was found that they exist in an active and in an inactive form. The NHase activity in cells decreased over time, but was restored upon exposure of the cells to white light. Also, the purified inactive enzyme could be activated upon exposure to white light. However, the purified active enzyme did not lose activity over time.

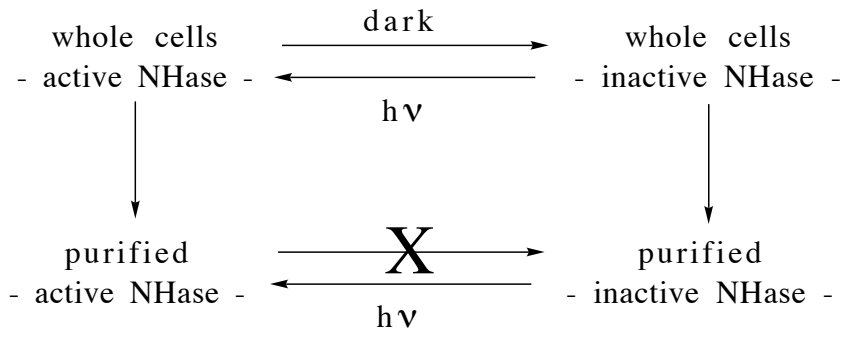


Figure 4. Activity Dependence of NHase.[28, 29]

Based upon the observed IR absorption of ^{14}N (natural abundance) labeled NHase (1855 cm^{-1}) as compared to ^{15}N labeled NHase (1820 cm^{-1}), it was proposed that NO (nitric oxide, nitrogen monoxide) is bound to the active site iron in the inactive form of NHase.[30] Subsequently, it was shown that light irradiation of inactive NHase produces NO and active NHase. The released NO was trapped by a spin trap that upon NO binding becomes EPR active.[31] In further studies active NHase was deactivated by the addition of NO gas.[31, 32] A detailed study showed that

active NHase can be inactivated by the addition of a NO solution or by NO produced *in situ* by NO-synthase.[33]

It was also found that butyrate inhibits NHase, but also stabilizes it.[36] This is important to consider when spectroscopic results are interpreted since NHase containing cells are often handled in butyric acid containing buffers. The author of this paper believes that butyrate forms a salt with one of the residues (*e.g.* Arg 56β in figure 5) in close proximity to the active center and/or within the channel connecting the active center to the surface of the protein. Thus, either the structure of the active center is disturbed or the access of the substrate to the active center is blocked. Thereby, the catalytic activity of NHase is reduced. However, when the crystal structure of NHase was solved no electron density corresponding to a butyrate ion was detected.[16] This can be due to the resolution of the crystal structure (2.65 Å) and/or due to the fact that the $\underline{H_3C\text{-}CH_2}\text{-}\underline{CH_2}\text{-}CO_2^-$ unit is very likely to be disordered. Also, the butyrate in the salt bridge is probably rapidly exchanging.

In the following paragraphs, a brief description of the development of the spectroscopic model of NHase will be presented. One should note that it was only during those studies that such concepts as low-pH/high-pH-form (*vide infra*), active/NO-inactivated form, with/without butyrate inhibitor were developed. Therefore, the earlier literature is sometimes difficult to comprehend in light of the information that is now available about NHase.

Since no substantial absorption bands were observed in the region 400-600 nm (Soret band = π-π* transition), it was concluded that NHase does not contain a heme unit.[22] Based upon the EPR[17] spectrum (g_{max} = 2.284, g_{mid} = 2.140, g_{min} = 1.971) it was concluded that active NHase contains a low-spin Fe^{3+} in its active center. The observed g values indicated

that no iron-sulfur clusters are present in NHase.[17] The relatively small value[17] for g_{max} - g_{min} (0.313) suggested that the iron center is ligated by a cysteine thiol. Since the EPR lines broadened[17] when isotopically enriched water was used, it was concluded that water is bound to the active site iron. This means that the coordination environment of the active site iron includes an open coordination site. In this open coordination site either water, substrate, or inhibitor can be bound. In agreement with this, it was found that azide inhibits the catalytic activity of NHase and perturbs its EPR spectrum.[17, 37] Resonance Raman results suggested that the absorption band at around 700 nm of active NHase, see figure 9, is due to "sulfur-to-iron-charge-transfer" (ref. 38, p. 334-336).[15a] Iron K-edge x-ray absorption spectroscopy of active NHase confirmed the coordination of sulfur to the iron center.[15a] The EXAFS data was fitted to 2.5 nitrogen or oxygen scatterers at 1.98 Å and 2.5 sulfur scatterers at 2.21 Å distance from the active site iron in active NHase.[15a] EXAFS measures n and r with an accuracy of ± 1 and ± 0.03 Å, respectively.[15a]

The equilibrium between inactive and light-activated NHase was investigated by Mössbauer spectroscopy, EPR, and magnetic susceptibility studies.[34] It was concluded that inactive NHase contains one low-spin Fe^{2+} and one low-spin Fe^{3+}, while both iron centers in active NHase are low-spin Fe^{3+}. Based upon later results it must be concluded that the inactive NHase used in those studies was in fact 'half-activated'.

ENDOR data indicated that the iron center in active NHase is in a N_3OS_2 coordination sphere involving three histidine imidazole nitrogens and water.[39] A further resonance Raman study 'suggested that amide nitrogens from the peptide backbone are participating in the observed modes', nevertheless only imidazole nitrogens were considered to be coordinated to the metal center.[40] It was concluded that the active site

iron is in the coordination environment as shown in figure 2.[40] In this study it was also recognized that active NHase is active at pH = 7.3 ('low-pH' form), but inactive at pH = 9 ('high-pH' form). Note, that the inactive high-pH form is not the NO-inactivated form. It was further shown that active NHase does not contain NO.[40] This resonance Raman data[40] showed that more than one Fe-S bond must be present and that considerable structural changes (*e.g.* reduction in number of hydrogen bonds around the active center) must be occurring when going from the low-pH to the high-pH form. From the relative energies of the vibrational modes in this resonance Raman data[40] it was concluded that the average Fe-S bond is 10 % stronger in the high-pH form as compared to the low-pH form.

In agreement with this conclusion, EXAFS analysis of the iron K-edge x-ray absorption spectrum indicated that one or two Fe-S bonds are shortened by 0.02 Å when going from the low-pH to the high-pH form.[41] The EXAFS fit is consistent with either two or three Fe-S bonds to a six-coordinated iron center.[41] Since the shortest Fe-x bond in the EXAFS analysis was 1.90-1.99 Å long, it was confirmed that no NO could possibly be bound to the Fe center in active NHase.[41,42] It was proposed that the S ligands in NHase are in a *cis* arrangement since the refined Fe-S bond lengths (2.19 - 2.21 Å) in the EXAFS analysis[41] are matching the Fe-S bond lengths (2.203(5) Å) in a Fe(III) model compound[26a] that contains two S ligands in a *cis* arrangement. Typically, the average Fe-S bond length in an Fe(III) complex containing two S ligands in a *trans* arrangement is 2.33 ± 0.05 Å.[41] The authors[41] concluded that "(1) the ligand set is N_3S_2O." "(2) The two sulfur ligands are" *cis* "thiolates". "(3) At least one and more likely two or three of the nitrogen ligands ... are from histidine side chains". "(4) ... The oxygen ligand to the iron is

solvent exchangeable, and almost certainly an aqua or hydroxo ligand. ... (5) The change in spectral properties of nitrile hydratase as pH is increased above 8 is associated with a shortening of one or both Fe-S bonds. ... The most likely explanation for this is loss of a hydrogen bond to a thiolate sulfur."

Recently, an iron K-edge x-ray absorption study of NO-inactivated NHase was undertaken.[43] Herein the 1:1 stoichiometry of NO bound to low-spin Fe(III) is confirmed.[30] This study will be discussed in chapter 6.

The crystal structure of NHase from *Rhodococcus* sp. R312 was recently solved by x-ray diffraction analysis.[16] Data up to a resolution of 2.65 Å was included in the refinement, the final model has R = 26.4 % and R_{free} = 28.9 %. The enzyme crystallized as an αβ heterodimer, see figure 5, with an extensive interface between two heterodimers, suggesting that in solution an $\alpha_2\beta_2$ tetramer might be in equilibrium with the αβ heterodimer. The active center is located within the conserved sequence[15] -Cys-Thr/Ser-Leu-Cys-Ser-Cys-Tyr/Thr- on the α subunit. The ligands to the iron ion are the thiolates of Cys 110 (axial), Cys 113, and Cys 115 and the peptide amide nitrogens of Ser 114 and Cys 115, see figure 5 for details. "These five ligands are located at five vertices of an octahedron, with the sixth position unoccupied".[16] EPR[17] and ENDOR[39] experiments indicated that an exchangeable water molecule is bound to the iron center. Given the resolution of the crystal structure, it is understandable that no electron density corresponding to a coordinated water molecule was detected. The discrepancy between the result of the x-ray crystallographic study and the result of EPR, EXAFS, ENDOR, and resonance Raman studies can be explained by the proposed mechanism of NHase as discussed in chapter 3.

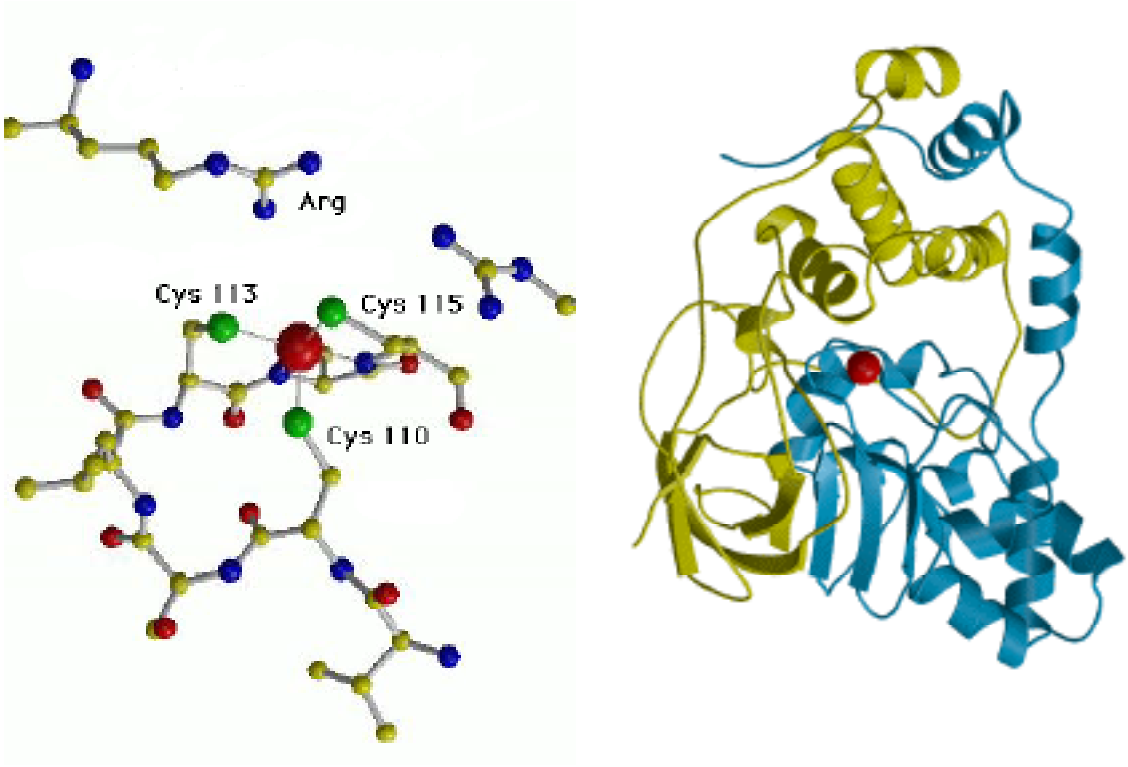


Figure 5. View of the Active Center of Nitrile Hydratase and Ribbon Diagram of the αβ Heterodimer (Fe = Red Sphere, α Subunit = Blue, β Subunit = Yellow).

bond	**distance (Å)**
Fe - S (Cys 113 or Cys 115)	2.1
Fe - S (Cys 115 or Cys 113)	2.3
Fe - S (Cys 110)	2.5
Fe - N (amide, Ser 114 or Cys 115)	1.9
Fe - N (amide, Cys 115 or Ser 114)	2.0
N-Arg 56β - Fe	3.3
N-Arg 56β - S (Cys 113 or Cys 115)	3.3
N-Arg 56β - S (Cys 115 or Cys 113)	3.6
N-Arg 56β - S (Cys 110)	6.0

Table 1. Selected Structural Parameters of Crystalline NHase.[27]

The active center of nitrile hydratase is unusual. There is only one other enzyme, the P-cluster of nitrogenase[7], in which coordination of an amide nitrogen to a metal center has been observed. Based upon the crystal structure it cannot be said whether or not the amide nitrogen is deprotonated. However, studies on model compounds indicated that the coordination of deprotonated nitrogens, which are negatively charged, to Fe(III) significantly stabilize it.[21] Only a small number of model compounds involving a coordination of a deprotonated carboxamido nitrogen to a metal have been reported.[21]

In one study[44] it was proposed that the oxygen of cysteine-sulfinic acid is coordinated to the active site iron in NHase. The authors concluded that Cys 112, which corresponds to Cys 113 in the crystal structure, is post-translationally oxidized to a cysteine-sulfinic acid (Cys-SO_2H) which is coordinated via one of its sulfinic acid oxygens to the iron. Thus far, no other authors have provided evidence for such a coordination mode. Therefore, it might be that in this study a partially oxidized enzyme was used.

It should be mentioned that about ten iron complexes containing *cis* sulfurs in a N_4S_2 donor set have been synthesized.[26,21] Some of them model the spectroscopic and electronic properties (UV/vis, EPR) of the active center of NHase surprisingly well. Furthermore, they also provide significant stabilization to the Fe(III), *id est* reduce the $E_{1/2}$ of the Fe(III)/Fe(II) redox couple.

It should also be noted that nitrilases and amidases do not require any metal ion to exercise their catalytic activity. Using mutagenesis studies it was shown that nitrilases and amidases require a cysteine residue to be catalytically active.

3.) Proposed Mechanism of Hydration of Nitriles to Form Amides by Nitrile Hydratase:

The author of this paper proposes that the nitrile hydratase catalyzed hydration of nitriles to form amides occurs by the mechanism shown in figure 6. This proposed reaction scheme provides an explanation of the previously suggested active site structures, namely, a $N_2S_3O_1$ and a $N_3S_2O_1$ coordination environment. Upon protonation the active center is converted from the $N_2S_3O_1$ coordination environment (**A**), as observed by x-ray crystallography, to the $N_3S_2O_1$ coordination environment (**B**), as proposed from EPR, EXAFS, ENDOR, and resonance Raman measurements. It is suggested that the axial cysteine, Cys 110, is protonated and the arginine above the open coordination site binds to the iron. Thus, the position of the open coordination site shifts. In the newly generated open coordination site the nitrile can then bind to form **C**. Thereby, the nitrile is activated for nucleophilic attack.[45] Cysteine 110 is now available to attack the coordinated nitrile. The thioimidate intermediate (**D**) reacts with water to form **E**. Under release of cysteine the coordinated amide derivative (**F**) is generated. It is in equilibrium with free amide and the **B** form of the enzyme.

This proposed mechanism is in agreement with the pH dependency of the enzyme activity. Nitrile hydratase is inactive at pH = 9, but active at pH = 7.3.[40] Note, that also in nitrilase[10], in a mutant of asparagine synthetase B[20], and in a mutant of the cysteine protease papain[35] an attack of a cysteine upon the nitrile is involved in the catalytic cycle. It is also known that nitriles that are activated by electron withdrawing groups are hydrated to the corresponding amides by catalysis of 2-mercaptoethanol in an aqueous phosphate buffer at pH = 9.[12] The proposed binding of the nitrile to the metal center prior to

the nucleophilic attack by the sulfur of cysteine is in agreement with the long known fact that the base hydrolysis of a nitrile to form an amide is accelerated by a factor of 10^6 upon coordination of the nitrile to a metal center.[13] It was also shown[17] that the EPR spectrum of native NHase changes upon mixing with propionitrile, which is a good substrate. After several minutes the original EPR spectrum is restored. The observed change in the EPR spectrum might be due to nitrile coordination to the active site iron.

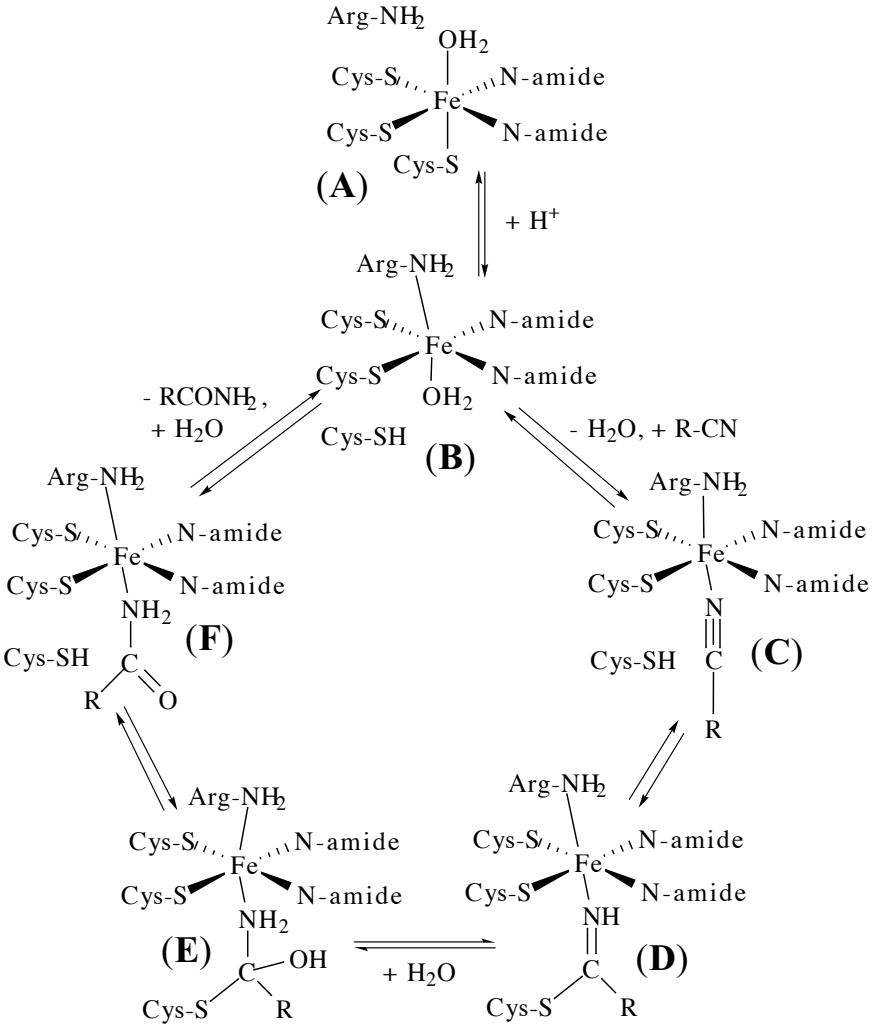


Figure 6. Proposed Catalytic Cycle of Nitrile Hydratase.

4.) Challenges of Modeling Low-spin Fe(III) in a N/S Coordination Environment:

The synthesis of compounds containing a low-spin Fe(III) in a sulfur coordination environment provides several challenges. Firstly, "the combination of Fe(III) and thiolates is thermodynamically unstable with respect to Fe(II) and disulfide formation."[46] This is a redox reaction followed by a radical recombination. The energy released in the reaction of two RS• radicals to form disulphide is the major driving force of this reaction. In agreement with this, it has been observed that in the synthesis of these compounds a relatively large amount of side-products is formed.[47] The compounds should, whenever possible, be stored at a low temperature, preferably as a solid, since they are unstable in solution.[59]

Secondly, compounds containing Fe-SR groups are susceptible to oxidation by oxygen present in the air. This could, for example, result in the formation of disulphide and iron oxide. Also, sulfoxide (-SO-) and sulfone ($-SO_2-$) could be formed. Therefore, those compounds have to be handled in a glovebox under an atmosphere of nitrogen or argon to exclude oxygen.

Further, coordinatively unsaturated compounds containing thiolates, *e.g.* **1**, are unstable. They can oligomerization via thiolate bridges.

5.) A Model of the Active Center of the Intermediate Form of Nitrile Hydratase:[4]

In a recent study it was shown that upon photolysis of the NO-inactivated form of NHase NO is released. This process was monitored by Mössbauer spectroscopy and EPR[52] at 4.2 K. Thereby, a short-lived intermediate was observed. Interestingly, the spectral parameters of this

intermediate are remarkably similar to those of the five-coordinated compound **1** ([Fe(III)pr_2imine$_2$$Me_2$]$PF_6$). The Mössbauer parameters of **1** and the short-lived NHase intermediate are within the range typically expected for low-spin Fe(III) having a non-spherical electron distribution.[48] Magnetic susceptibility measurements of **1** indicate that below T = 100 K no spin states above S = 1/2 are thermally accessible.[37]

system parameter	nitrile hydratase - active enzyme		nitrile hydratase - intermediate	[Fe(III)pr_2imine$_2$ Me_2]PF_6 (**1**)
isomer shift - δ (mm/s)	0.24[4]	0.33[34]	0.27	0.21
quadrupole splitting constant - ΔE_Q (mm/s)	2.82[4]	0.37[34]	3.1	3.01

Table 2. Mössbauer Parameters of the Active Form and Intermediate Form of Nitrile Hydratase and of Compound **1**.

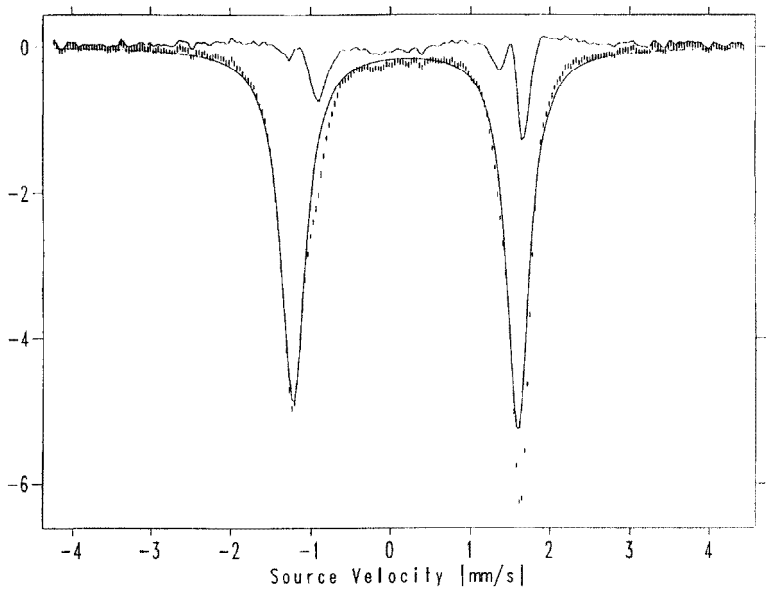


Figure 7. Mössbauer Spectrum of 95% Pure [Fe(III)pr_2imine$_2$$Me_2$]$PF_6$ (**1**) (T = 4.2 K, B = 0 G, ^{57}Fe Natural Abundance).

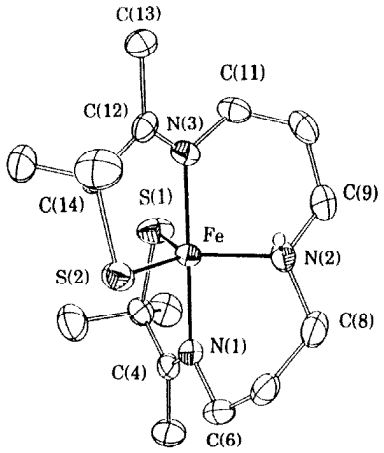


Figure 8. ORTEP of $[Fe(III)pr_2imine_2Me_2]PF_6$ (**1**).[37]

	$[Fe(III)pr_2imine_2Me_2]PF_6$ (**1**)[37]	$[Fe(II)pr_2imine_2]$ • EtOH (**3**)[49]
Fe-S(1)	2.133(2) Å	2.363(1) Å
Fe-S(2)	2.161(2) Å	2.342(1) Å
Fe-N(1)	1.967(4) Å	2.168(3) Å
Fe-N(3)	1.954(4) Å	2.183(4) Å
Fe-N(2)	2.049(4) Å	2.181(3) Å
N(1)-Fe-N(3)	178.1(2)°	167.7°
S(1)-Fe-S(2)	121.0(1)°	124.3°
S(2)-Fe-N(2)	106.5(1)°	114.0(1)°
S(1)-Fe-N(2)	132.3(1)°	121.6°
N(1)-Fe-S(1)	86.7(1)°	82.9(1)°
N(1)-Fe-S(2)	95.2(1)°	104.7(1)°
N(1)-Fe-N(2)	94.2(1)°	87.6(1)°
N(3)-Fe-S(1)	91.6(1)°	101.7(1)°
N(3)-Fe-S(2)	86.4(1)°	82.3(1)°
N(3)-Fe-N(2)	86.2(1)°	80.3(1)°

Table 3. Selected Structural Parameters of **1** and **3**.

In table 3 selected structural parameters of [Fe(III)pr$_2$imine$_2$Me$_2$]PF$_6$ (**1**) and, for comparison, of [Fe(II)pr$_2$imine$_2$] (**3**) are given. Compound **3** is similar to compound **1**, except that the iron is reduced to Fe(II) and the two α-methyl groups are not present in the ligand.

Because of the similarity of the Mössbauer parameters and EPR parameters[52] (g_{max} = 2.201, g_{mid} = 2.146, g_{min} = 2.001) of **1** and those of the short-lived NHase intermediate, one can describe **1** as being a spectroscopic model of the short-lived NHase intermediate. Since there is a similarity between the spectroscopic data, one can expect that the structural parameters and the coordination sphere (N_3S_2) of **1** resemble those of the short-lived NHase intermediate. Note, that **1** is a five-coordinated compound, meaning that it has one open coordiantion site. Therefore, the short-lived NHase intermediate contains a five-coordinated Fe(III) having an open coordination site. If the bound NO dissociates off the six-coordinated active site iron, then, for a short time, the five-coordinated intermediate is present.

Hence, it is possible to synthesize a 'small' compound, which is a structural model of an intermediate in an enzyme reaction. This is a very fascinating aspect of this research! Note, also the similarities between the structural and spectroscopic parameters of **2** and those of the NO-inactivated enzyme, as discussed in chapter 6.

It is further important to mention that compound **1** was originally intended to be a structural model of the 'spectroscopically' determined structure of the active center of NHase (see figure 2 on page 8 for details). Interestingly, **1** models also one of its electronic properties (*id est* low-spin (S = 1/2) Fe(III)).

6.) A Model of the Active Center of the NO-Inactivated Form of Nitrile Hydratase:[5]

As it was mentioned above, NHase exists in an active and in an inactive form. The inactive form was found to be formed by the binding of NO to the active center of active NHase. NO binding and release, thus, regulates the activity of NHase.

Within the last several years a constantly increasing number of biological functions of NO have been found.[50] They include the regulation of blood pressure by NO. NO binds to the iron in the heme group of guanylate cyclase, thus causing a conformational change which activates guanylate cyclase. Guanylate cyclase is then converting GTP (guanosine triphosphate) into cGMP (guanosine 3',5'-monophosphate). cGMP acts as a secondary messenger molecule to active protein kinases which ultimately results in the relaxation of smooth muscle, thus widening the blood vessel. NO acts further as a neurotransmitter and is produced as part of the immune response mediated by macrophages. Here, the function of NO is to inhibit enzymes of the antigen (*e. g.* invading bacteria) and to cause destructive radical reactions.

NO is produced in biological systems by the enzyme NO synthase, a heme protein. It converts L-Arg to citrulline and NO in a five-electron oxidation process that requires O_2 and NAPDH (reduced nicotinamide adenine dinucleotide phosphate).

The NO-inactivated form of NHase is EPR silent, therefore it does not possess an odd number of unpaired electrons. It has an absorption maximum at 370 nm, see figure 9 for details. Its Mössbauer parameters are given in table 4. EXAFS analysis indicated the bond lengths shown in table 5.

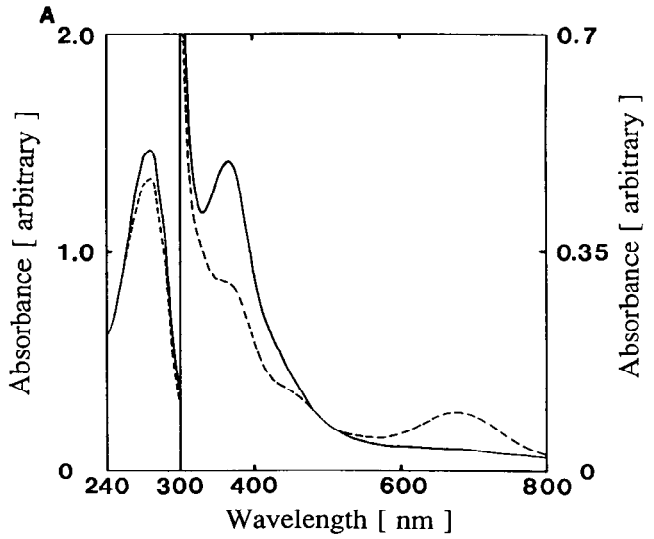


Figure 9. Absorption Spectrum of Active (---) and Inactive (*f*) NHase.

system parameter	nitrile hydratase - NO-inactive enzyme -		[Fe(III)pr$_2$imine$_2$Me$_2$(NO)] PF_6 (**2**)
isomer shift - δ (mm/s)	0.05[5]	0.02[34]	0.0924
quadrupole splitting constant - ΔE_Q (mm/s)	1.5[5]	1.49[34]	1.0078

Table 4. Mössbauer Parameters of the NO-Inactive Form of Nitrile Hydratase and of Compound **2**.

	nitrile hydratase - NO-inactive enzyme -		[Fe(III)pr$_2$imine$_2$ Me$_2$(NO)]PF_6 (**2**)
$n_{NO}/n_N/n_S$	1/2/3	1/3/2	1/3/2
r(Fe-NO) (Å)	1.687(16)	1.692(15)	1.674(15)
r(av. Fe-N) (Å)	1.970(15)	1.976(11)	2.003(21)
r(av. Fe-S) (Å)	2.265(7)	2.268(7)	2.255(11)
∠Fe-N-O (°)	164	166	167

Table 5. EXAFS Parameters of the NO-Inactive Form of Nitrile Hydratase and of Compound **2**.

	[Fe(III)pr_2imine$_2$$Me_2$(NO)]$PF_6$ (**2**)
Fe-S(1)	2.2603(9) Å
Fe-S(2)	2.2604(9) Å
Fe-N(1)	1.993(3) Å
Fe-N(3)	1.979(3) Å
Fe-N(2)	2.108(3) Å
Fe-N(4) (NO)	1.676(3) Å
N(4)-O(1) (NO)	1.161(4) Å
S(2)-N(2)	3.064(3) Å
S(2)-HN(2)	2.613(1) Å
Fe-N(4)-O(1)	172.3(3) °
N(1)-Fe-N(3)	165.92(11) °
S(1)-Fe-S(2)	91.09(3) °
S(2)-Fe-N(2)	89.02(7) °
S(1)-Fe-N(2)	174.29(8) °
N(1)-Fe-S(1)	84.68(8) °
N(1)-Fe-S(2)	83.57(8) °
N(1)-Fe-N(2)	101.01(11) °
N(3)-Fe-S(1)	91.35(8) °
N(3)-Fe-S(2)	83.01(8) °
N(3)-Fe-N(2)	83.00(11) °
C(1)-S(1)-Fe	100.50(11) °
C(10)-S(2)-Fe	100.91(10) °

Table 6. Selected Structural Parameters of **2**.

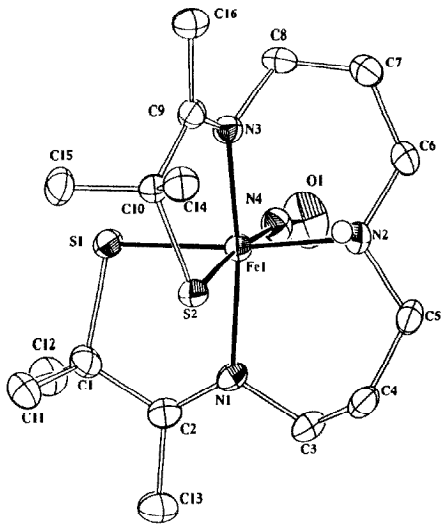


Figure 10. ORTEP of [Fe(III)pr_2imine$_2$$Me_2$(NO)]$PF_6$ (**2**).

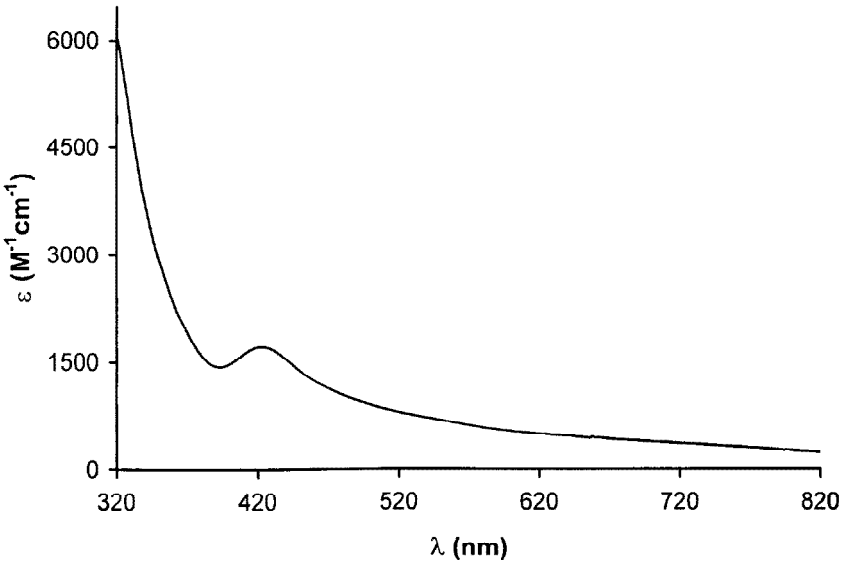


Figure 11. Absorption Spectrum of [Fe(III)pr_2imine$_2$$Me_2$(NO)]$PF_6$ (**2**).

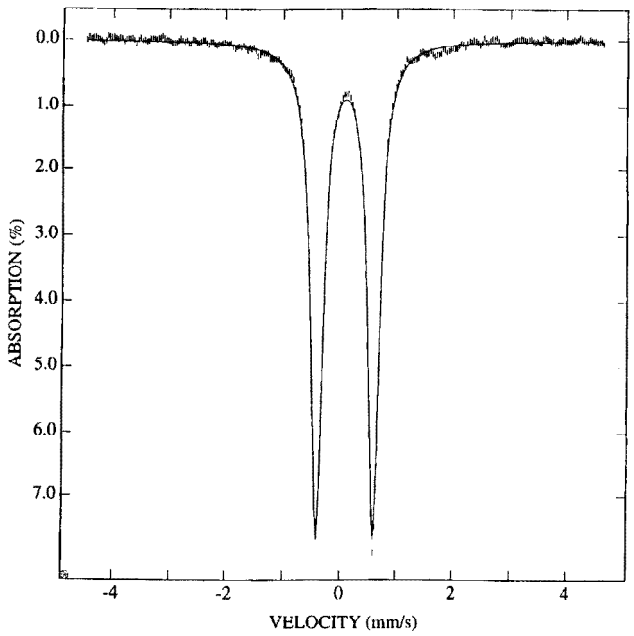


Figure 12. Mössbauer Spectrum of 100% Pure [Fe(III)pr_2imine$_2$$Me_2$(NO)] PF_6 (**2**) (T = 4.2 K, B = 0.5 kG, ^{57}Fe Natural Abundance).

As discussed above, compound **1** proved to be a good model of the intermediate form of NHase. Furthermore, **1** also matched the spin state of active NHase. Therefore, it was decided to investigate if compound **1** can react with NO. An inspection, see table 3, of the crystal structure of **1** shows the S(1)-Fe-N(2) angle to be 'open' (132.3(1)$^{-}$). Normally, in a ideal trigonal bipyramidal coordination environment, one expects this angle to be 120^{-}. It was expected that NO will bind through this angle to the Fe center. Note, that the S(1)-Fe-N(2) angle is opposite to the hydrogen atom on N(2). It was hoped that NO will bind to the Fe in **1** in a fashion that resembles the binding mode of NO to the active site Fe of NHase. If this is the case then the structural and electronic properties of the **1**-NO adduct should match those of the NO-inactivated form of NHase. One could then investigate the structural and electronic properties of the **1**-NO adduct, the analogue of the NO-inactivated NHase, at a level of detail which is impossible to achieve in enzymes.

It was found that the reaction of **1** with 1.15 equivalents of NO results in the formation of a NO adduct of **1** (for synthetic details see chapter 8). This compound proved to be $[Fe(III)pr_2imine_2Me_2(NO)]PF_6$ (**2**). Its ORTEP and some of its structural parameters are given in figure 10 and table 6, respectively. A comparison of the structural parameters of **2** as determined by EXAFS, see table 5, and by x-ray crystallography, see table 6, shows that both are very similar. This shows that EXAFS can provide accurate structural information.

If one compares figure 9 and figure 11, one realizes that the absorption spectrum of **2** matches the one of NO-inactivated NHase very closely. Within the range 320 - 800 nm^{-1} NO-inactivated NHase and **2** each have single absorption maximum at 370 and 422 nm^{-1}, respectively. "The electronic band at 370 nm ... of inactive NHase" is "due to ... transitions" containing "both ... Fe←NO and Fe←S charge transfer character".[32] ^{14}N-NO-inactivated NHase (natural abundance) has a ν_{NO} of 1853 cm^{-1} (with ^{15}N-NO, ν_{NO} = 1818 cm^{-1})[32], while **2** has a ν_{NO} of 1820 cm^{-1} (^{14}N, natural abundance, see figure 26 in chapter 8 on page 50).

As it is shown in table 4, the Mössbauer parameters of **2** and of the NO-inactivated form of NHase are very similar. They fall in the range expected for a low-spin Fe(II) or Fe(III) in a very unsymmetrical electron environment.[48] Table 5 shows that the structural parameters as determined by EXAFS of NO-inactivated NHase are also very similar to those of **2**. However, it also shows that EXAFS could fit both a $N_2S_3(NO)$ coordination environment and a $N_3S_2(NO)$ coordination environment to the measured data of NO-inactivated NHase.

Compound **2** is formed by the reaction between Fe(III) and NO•. Therefore it is an $\{FeNO\}^6$ complex.[54,55] $\{FeNO\}^6$ means that a total

number of 6 electrons is associated with the iron d and the NO π* orbitals. An $\{FeNO\}^6$ complex can formally be composed of 'Fe(II) and NO^+', 'Fe(III) and NO•', or 'Fe(IV) and NO^-'. One could say that the $\{FeNO\}^6$ unit is composed of those three resonance structures. "The bonding in the $M(NO)_x$ moieties of metal nitrosyl complexes is largely of a covalent nature, and ... the electron distribution in the M-NO unit is more or less evenly distributed in this group. As a result, it is unreasonable to assign formal oxidation states to the metal and the nitrosyl ligand in M-NO complexes."[54]

$[Fe(III)pr_2imine_2Me_2(NO)]PF_6$ (**2**) is diamagnetic as shown in the NMR figures in chapter 8 on page 48 and 49, this was also shown by EPR measurements[51]. Since **1** and NO• each have a spin of 1/2, an electron pairing must be occurring upon formation of **2**. Therefore, the Fe-NO bond must have a partial double bond character. This partial double bond character is expressed in the considerably shorter Fe-NO bond length (1.676(3) Å), as compared to the other Fe-N bonds (mean: 2.0(1) Å) in **2**. The Fe-NO distance in **2** falls within the range (1.62 - 1.68 Å) expected for $\{FeNO\}^6$ systems.[42] A MO explanation for the spin pairing is given in chapter 7. The MO in which this newly formed electron pair is located is distributed throughout the molecule.

	NO^+	NO•	NO^-	'NO' in inactive NHase	'NO' in **2**
r(N-O) (Å)	1.06	1.15	1.26	N/A	1.161(4)
ν_{N-O} (cm^{-1})	2377	1875	1470	1853	1820

Table 7. Comparison of 'NO' Parameters.[54,57]

The IR data for both **2** and NO-inactivated NHase fall into the range expected for an $\{FeNO\}^6$ system.[57] A comparison of the data in

table 7 suggests that the dominant resonance structure in both NO-inactivated NHase and **2** is 'Fe(III)-NO•'. Based upon the fact that NO-inactivated NHase is formed by the reaction[33] between NHase (Fe(III)) and NO, and based upon the similarities (UV/vis, IR, magnetism, EXAFS, and Mössbauer) between **2** and NO-inactivated NHase, the Fe-NO moiety in NO-inactivated NHase is assigned as being {FeNO}^{6}.[43] Also, the ∠ Fe-N-O in **2** is nearly linear (172.3(3)$^{-}$), therefore it is expected that this angle in NO-inactivated NHase is also nearly linear.

NHase binds NO reversibly. However, compound **2** does not bind NO reversibly. It was not possible to observe any formation of **1** when **2** was exposed to light and/or stored at room temperature for several days. The following experiments, all, except the EPR study, at room temperature, have been performed. When solid **2** was exposed to light no formation of **1** or decomposition of **2** was observed by EPR.[51] An unidentified diamagnetic ^{1}H NMR spectrum was observed in a sample of **2**, which was stored as a CD_3CN solution in the dark for two weeks in a closed NMR tube.[58] Irradiation (UV/vis) of a CD_3CN solution of **2** in a closed NMR tube for two hours showed the presence of another unidentified diamagnetic ^{1}H NMR spectrum.[58] Compound **2**, in a MeCN solution under a N_2 atmosphere in the dark, showed considerable decomposition after four hours, as judged by UV/vis spectroscopy.[58] Irradiation (UV/vis) of a CH_3CN solution of **2** under a N_2 atmosphere showed decomposition of **2** within three hours, as judged by UV/vis spectroscopy.[58] Further, it was shown that **1** in a MeCN solution does not significantly decompose within two weeks if stored in the dark.[58,59] However, exposure of a MeCN solution of **1** to UV/vis radiation causes considerable decomposition within four hours.[58] From these results it

must be concluded that the photolytic cleavage of **2** in solution to form **1** and NO may be not be observable, since the product **1** decomposes under UV/vis irradiation.

Compound **2** contains Fe in a $N_3S_2(NO)$ coordination environment. Because of the similarities between **2** and NO-inactivated NHase, one might suspect that the Fe in NO-inactivated NHase is also in a $N_3S_2(NO)$ coordination environment. This would mean that NO binds to structure **B** of NHase, see the proposed mechanism in chapter 3. It would be interesting to compare the parameters of an $\{FeNO\}^6$ compound that contains Fe in a $N_2S_3(NO)$ coordination environment (model of structure **A**) to the parameters of **2** and NO-inactivated NHase. This would further help to assign a correct coordination environment to the active site Fe in NO-inactivated NHase.

Another six-coordinated derivative of **1** has been synthesized. It is $Fe(III)pr_2imine_2Me_2(N_3)$ (**4**)[37] in which azide is bound to the iron center through the S(1)-Fe-N(2) angle, as NO does. The Fe in **4** is in the low-spin (S = 1/2) state. A comparison of corresponding bond lengths in **2** and **4** shows the Fe-S bonds in **2** to be slightly (0.06 Å) elongated and the Fe-N(2)amine bond in **2** to be slightly shortened (0.05 Å). This can be explained if one assumes, like it is done in the discussion in chapter 7, that the orbital 'yz', *vide infra*, which contains the unpaired electron in **1**, which pairs with the unpaired NO π* electron, has σ* Fe-S character. "The resulting doubly occupied MO would thus be bonding with respect to Fe-NO, but slightly antibonding with respect to Fe-S and N-O. The weaker interaction between S and Fe would decrease the sulfur's trans influence resulting in a stronger interaction between N(2) and Fe, and

thus a shorter Fe-N(2) bond."[5] Note, that the Fe-N(1,3)imine distances in **1**, **2**, and **4** are very similar.

	Fe(III)pr_2imine$_2$$Me_2$($N_3$) (**4**)[37]
Fe-S(1)	2.196(1) Å
Fe-S(2)	2.209(1) Å
Fe-N(1)	1.978(3) Å
Fe-N(3)	1.970(3) Å
Fe-N(2)	2.157(3) Å
Fe-N_3 (azide)	2.061(4) Å

Table 8. Selected Structural Parameters of Fe(III)pr_2imine$_2$$Me_2$($N_3$) (**4**).[37]

7.) Electronic Structure of Model Compounds:

In order to be able to give a molecular orbital (MO) description a coordinate system has to be defined. The coordinate system which was chosen for the $[Fe(III)pr_2imine_2Me_2]^+$ ion is shown in the next figure. For the $[Fe(III)pr_2imine_2Me_2(NO)]^+$ ion a coordinate system was constructed in which the NO ligand binds along the y axis. By using the y axis for the NO ligand the coordinate systems of $[Fe(III)pr_2imine_2Me_2]^+$ and of $[Fe(III)pr_2imine_2Me_2(NO)]^+$ are as similar as possible. Note that both ions are of C_1 symmetry.

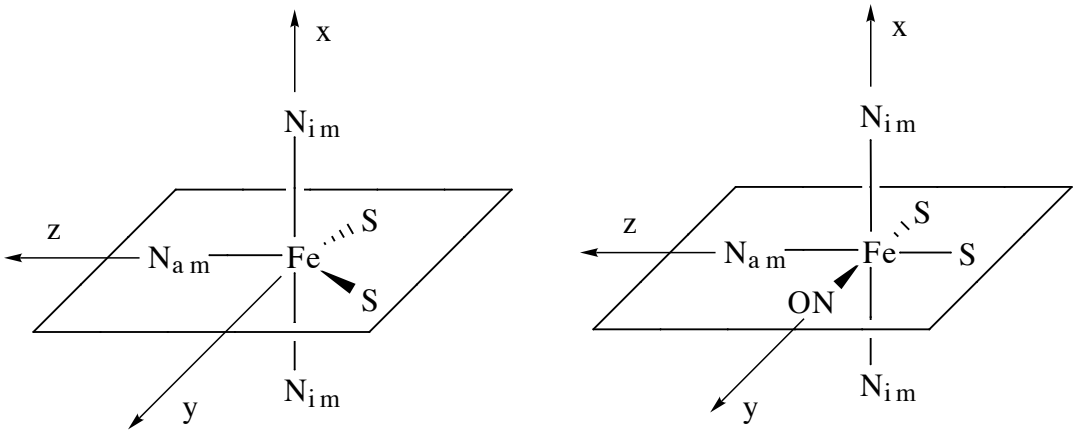


Figure 13. Coordinate Systems for $[Fe(III)pr_2imine_2Me_2]^+$ and for $[Fe(III)pr_2imine_2Me_2(NO)]^+$.

Herein, an abbreviated qualitative molecular orbital description is presented. Since both imine nitrogens and both sulfurs are in an identical chemical environment, it cannot be assumed that only one metal orbital interacts with only one ligand orbital. In a detailed qualitative molecular orbital diagram one would have to construct mixed metal orbitals so that both metal-imineN and both metal-S interactions are equivalent. The level of approximation chosen for the

MO diagrams is sufficient to explain the spin of 1/2 of $[Fe(III)pr_2imine_2Me_2]^+$ and to explain the spin-pairing upon binding of NO to $[Fe(III)pr_2imine_2Me_2]^+$. Density function calculations, which will provide a quantitative description of the shapes and energies of the molecular orbitals of $[Fe(III)pr_2imine_2Me_2]^+$, are currently in progress in the research group of Professor Solomon at Stanford University.

7.1.) Abbreviated Qualitative Molecular Orbital Diagram of the $[Fe(III)pr_2imine_2Me_2]^+$ Ion:

In the MO diagram of $[Fe(III)pr_2imine_2Me_2]^+$ only σ interactions are considered. Also, only the higher energy orbitals that are involved in bonding are considered. The atomic orbitals of iron, which are involved in bonding, are higher in energy than the atomic orbitals of the ligands, which are involved in bonding. Therefore, one can assume that the σ molecular orbitals have mainly ligand character while the σ* and non-bonding (n) molecular orbitals have mainly metal character. Thus, the molecular orbitals are denoted as, for example, 'yz', indicating that the molecular orbital 'yz' has approximately the same shape (angular dependence function) as the atomic orbital yz. In other words, the contributions of other atomic orbitals to the molecular orbital 'yz' are close to zero.

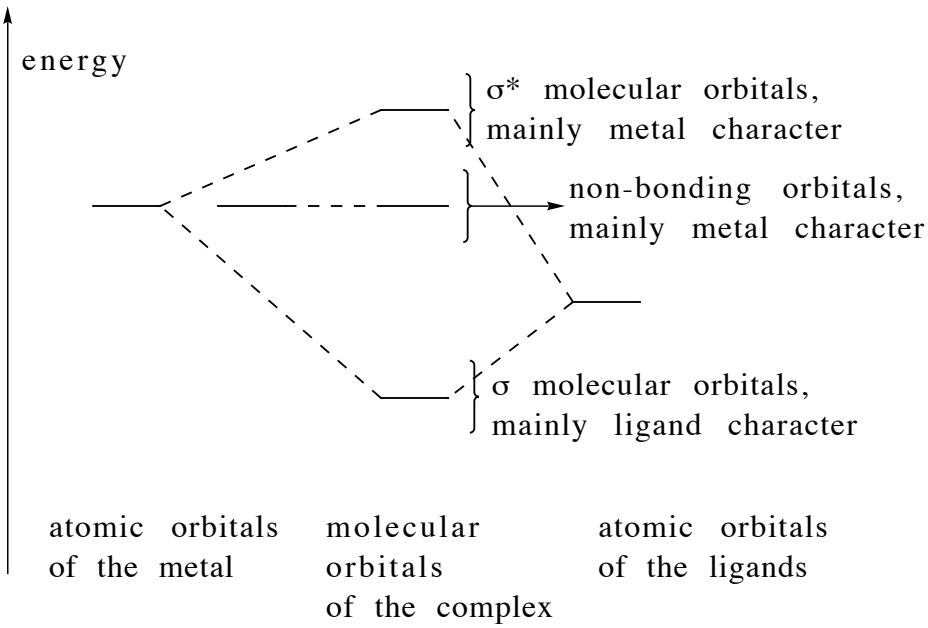


Figure 14. General Qualitative Molecular Orbital Diagram of a Metal Complex.

If one considers the orientations of the metal-based 3d and 4p orbitals within the coordinate system, one can conclude that the 'xy', 'xz', and 'y' molecular orbitals are non-bonding. This is the case since they are not directly pointing at any ligand. Likewise, since they are pointing at at least one ligand, one can conclude that the 'yz', 'z^2', 'x^2-y^2', 'z', and 'x' molecular orbitals are anti-bonding (σ*). Crystal field arguments indicate that the 'xz' orbital is higher in energy than the 'xy' orbital because the 'xz' orbital interacts in its plane with three ligands, while the 'xy' orbital interacts in its plane with only two ligands. Crystal field arguments further indicate the following order according to increasing energy: 'yz' < 'z^2' < 'x^2-y^2'. The 'x^2-y^2' MO is higher in energy than the 'z^2' MO, since 'x^2-y^2' points directly at two ligands, while 'z^2' points directly at only one ligand. The 'yz' MO is lower in energy since it only points indirectly at the two S ligands. Because the 4p atomic orbitals are higher in energy than the 3d atomic orbitals, the 'p'

molecular orbitals must also be higher in energy than the 'd' molecular orbitals. Since the molecular orbital 'y' is non-bonding, it must be lower in energy than the 'x' and 'z' molecular orbitals. The five σ molecular orbitals are completely filled using the ten electrons which are contributed by the ligands to the formation of bonds (2 imineN with 2 e^- each, 1 amineN with 2 e^-, and 2 S with 2 e^- each). Therefore, all five 3d e^- of Fe(III) are used to fill the 'd' molecular orbitals. This MO diagram explains the fact that $[Fe(III)pr_2imine_2Me_2]^+$ has a spin of S = 1/2, if one assumes that the energy difference between the 'xz' orbital and the 'z^2' orbital is larger than the spin pairing energy. Only the HOMO/LUMO region is shown in the MO diagram of $[Fe(III)pr_2imine_2Me_2]^+$.

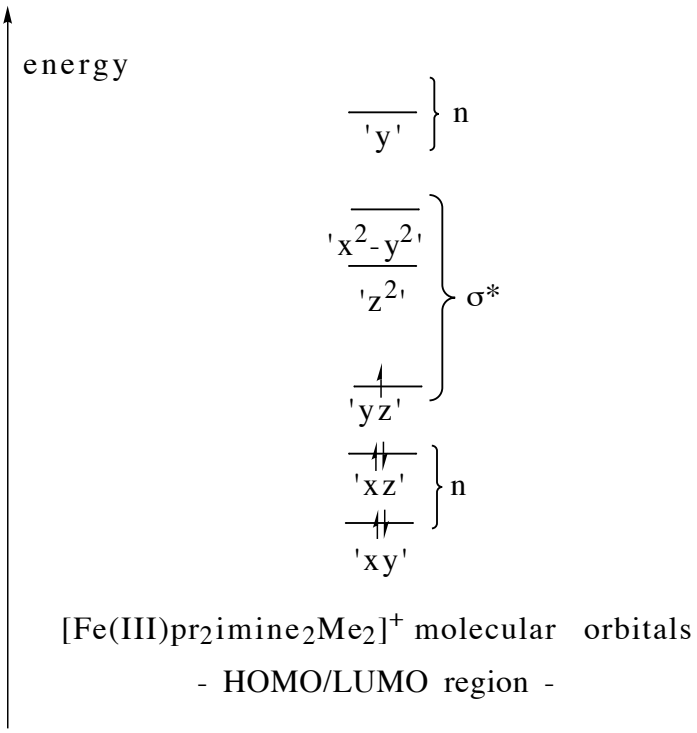


Figure 15. Abbreviated Qualitative Molecular Orbital Diagram (HOMO/LUMO region) of the $[Fe(III)pr_2imine_2Me_2]^+$ Ion.

7.2.) Abbreviated Qualitative Molecular Orbital Diagram of the $[Fe(III)pr_2imine_2Me_2(NO)]^+$ Ion:

For the NO to bind to the five-coordinated compound, $[Fe(III)pr_2imine_2Me_2]^+$, an empty non-bonding orbital must point in the direction of the incoming NO ligand. This condition is satisfied by the presence of the non-bonding 'y' orbital. Since for $[Fe(III)pr_2imine_2Me_2(NO)]^+$, S = 0, there must be spin pairing between the unpaired electron spin of $[Fe(III)pr_2imine_2Me_2]^+$ and of NO. This can be achieved either if the orbitals of $[Fe(III)pr_2imine_2Me_2]^+$ and NO that contain the unpaired electron interact to form two molecular orbitals or if antiferromagnetic coupling occurs. Since Fe and NO are adjacent, it is assumed that a π interaction between the $[Fe(III)pr_2imine_2Me_2]^+$ 'yz' σ* orbital and the NO π* orbital containing the unpaired electron occurs. This π interaction results in the formation of a new bonding and a new anti-bonding orbital between Fe and NO. Those two interactions are shown in the following MO diagram. Only the HOMO/LUMO region and the molecular orbitals of NO that are involved in M-NO binding are shown. The MO diagram of NO (see figure 18 on page 38) has been published.[54] About 60 % of the spin density of the unpaired electron is located on the N atom.[54] In a more detailed description of $[Fe(III)pr_2imine_2Me_2(NO)]^+$, one would have to consider a π interaction between the filled 'xy' orbital and the empty NO π* orbital. This would be called a π "back-bonding" or a π "back-donation".[38] A graphical representation of the formation of the σ and π bond between Fe and NO is shown in figure 17.

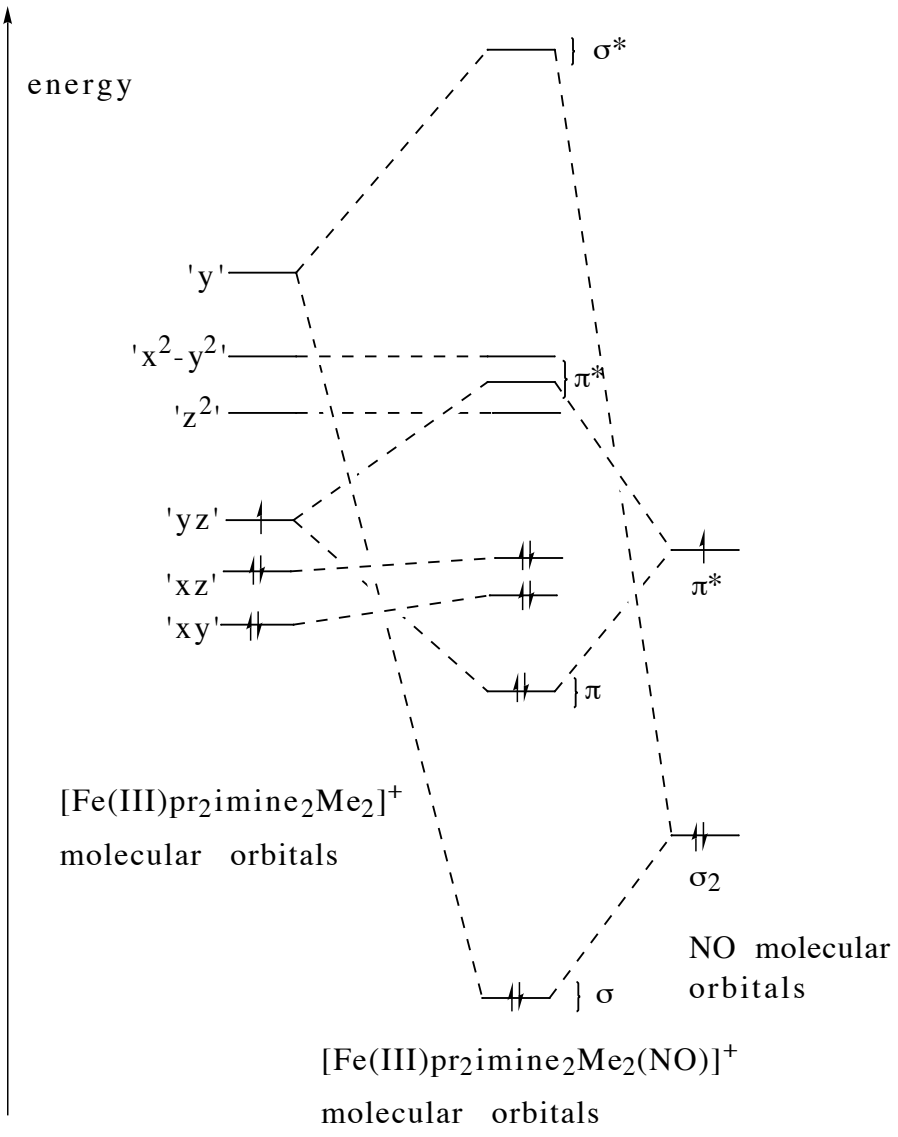


Figure 16. Abbreviated Qualitative Molecular Orbital Diagram of the $[Fe(III)pr_2imine_2Me_2(NO)]^+$ Ion.

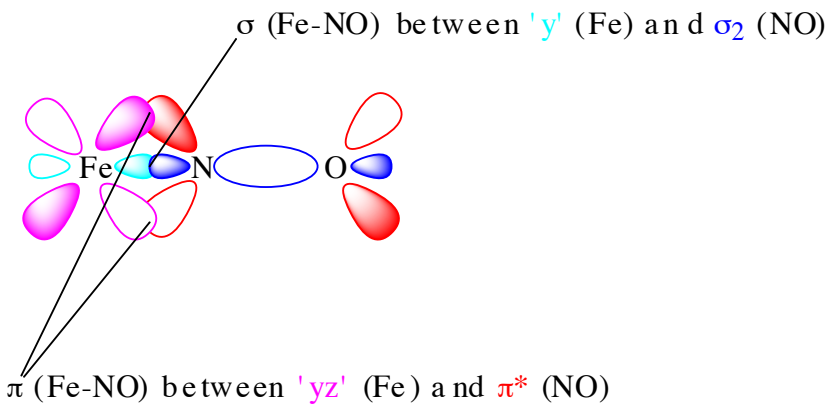


Figure 17. Graphical Representation of the Formation of a σ and a π Bond between Fe and NO.

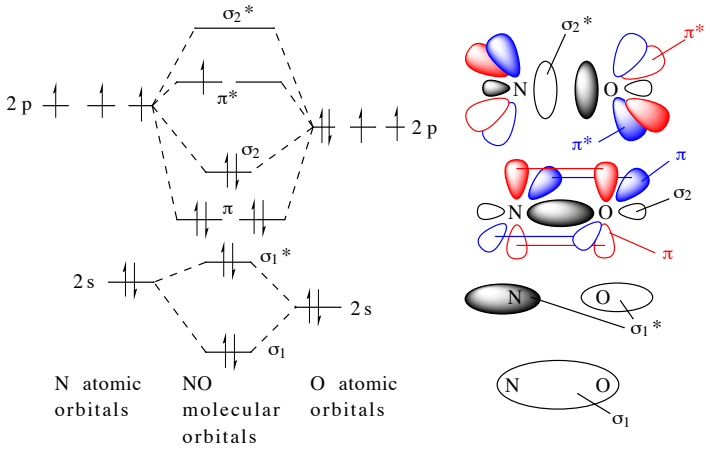


Figure 18. MO Diagram of NO.[54]

8.) Experimental Section:

Methods and Materials:

All reactions involving oxygen and/or water sensitive compounds were performed in a Vacuum Atmospheres dry box or on a high vacuum line using Schlenk techniques under dry nitrogen. In the dry box it proved to be useful to add solids to a flask via a funnel that fits through the joint into the flask. The balance boat and the funnel were thereafter

washed with the appropriate solvent. Generally in the dry box, liquid reactants were weighted out on the balance into a glass container. This glass container was then filled with approximately 1 ml of the appropriate solvent. The solution was mixed with a pipette and added to the flask. Then the glass vial was washed with 2 ml of solvent. In synthetic procedures this will be listed as "a g of b were added employing 3 ml of c". Stirring was always achieved by means of a magnetic stirring bar. All chemicals, except when stated otherwise, were used as received from commercial suppliers. $Fecp_2PF_6$ was synthesized according to a published procedure.[60] Solvents were dried before use. Sodium was added to methanol and it was then distilled under nitrogen. Acetonitrile was distilled from calcium hydride under nitrogen. Diethylether was vacuum transferred from sodium/benzophenone after the typical blue color was present.

Physical Measurements:

Infrared (4400 - 450 cm^{-1}) spectra were recorded on a Perkin Elmer 1600 FTIR instrument using samples pressed into a KBr pellet at circa 23 °C. Electronic (190 - 820 nm) spectra were recorded on a Hewlett Packard 8452A diode array spectrophotometer interfaced to a PC at circa 23 °C. ^1H NMR spectra were recorded on a Bruker AC200 at circa 23 °C. Chemical shifts are reported in ppm referenced to TMS, $\delta = 0.00$. Crystals suitable for x-ray diffraction analysis were suspended in paraffin oil in a glove box and then evaluated under a microscope. X-ray diffraction data were collected on a Nonius KappaCCD diffractometer using graphite-monochromated Mo Kα radiation ($\lambda = 0.71069$ Å) at a temperature of 161 K. The structure was solved by direct methods (SIR 92) and refined with SHELX97. For Mössbauer measurements (natural abundance, ~2.25

% ^{57}Fe) approximately 35 mg of substance were ground with 15 mg of BN in a mortar and placed into a Mössbauer sample holder. The sample was then shipped to Emory University for analysis. CV data in MeCN were collected in a cell using a 0.01 M $AgNO_3$ (containing 0.1 M electrolyte)/Ag electrode as the reference electrode, a platinum disc working electrode, and a platinum wire auxiliary electrode. As internal reference the redox couple $Fecp_2^{+/0}$ (0.003 M, + 0.1 M electrolyte) was used. But_4NPF_6 was used as the electrolyte. A Bioanalytical Systems, Inc. electrochemical analyzer interfaced to a PC was used in the measurements.

For $Fecp_2^{+/0}$ in MeCN, it was found $E_{1/2}$ = +86 mV versus 0.01 M $AgNO_3$/Ag. When a saturated KCl calomel electrode (SCE) ($E_{1/2}$ = +0.2412 mV versus NHE)[56] was used[61] as the reference electrode the $Fecp_2^{+/0}$ redox couple in MeCN had a $E_{1/2}$ = +400 mV. Thus, the measured $E_{1/2}$ versus 0.01 M $AgNO_3$/Ag ($E_{1/2}$ (Ag^+/Ag)) are converted into the $E_{1/2}$ versus SCE ($E_{1/2}$ (SCE)) by $E_{1/2}$ (SCE) = $E_{1/2}$ (Ag^+/Ag) + 314 mV. The $E_{1/2}$ versus NHE ($E_{1/2}°$) is obtained by $E_{1/2}° = E_{1/2}$ (Ag^+/Ag) + 555 mV. It was recommended by IUPAC[62] to report redox potentials obtained in non-aqueous solvents versus the $Fecp_2^{+/0}$ redox couple. To do this, the potential of the $Fecp_2^{+/0}$ redox couple is set to zero. The $E_{1/2}$ versus $Fecp_2^{+/0}$ ($E_{1/2}$ (Fc)) is calculated by $E_{1/2}$ (Fc) = $E_{1/2}$ (Ag^+/Ag) - 86 mV.

Synthesis of 3-chloro-3-methylbutanone-2 (**5**):

This compound was synthesized according to the procedure given in the literature[63] using predestilled sulfuryl chloride. Under nitrogen and cooling with ice/rocksalt sulfuryl chloride (0.6 mol) was added dropwise using a pressure equalized dropping funnel to a 500 ml three-necked flack containing stirred 3-methylbutanone-2 (0.6 mol). After the addition was completed the reaction was stirred for 12 hour at room

temperature. Upon destillation of the crude reaction mixture a clear colorless liquid was obtained (T_b = 24 °C / p = ~7 Torr). ^{1}H NMR spectroscopy indicated that less than 5 % impurities were present. The starting material 3-methylbutanone-2 accounted for most of the impurities. The ^{1}H NMR spectrum ($CDCl_3$) of 3-chloro-3-methylbutanone-2 (**5**) contains two peaks: 1.675 ppm [$CH_3COCCl(CH_3)_2$] and 2.374 ppm [$CH_3COCCl(CH_3)_2$]. The reaction performed on a 0.6 mol scale gave a reproducible isolated yield of 75 %.

Synthesis of 3-mercapto-3-methylbutanone-2 (**6**):

To synthesize this compound 3-chloro-3-methylbutanone-2 (**5**) was used in the reported procedure.[64] A with ice/rocksalt cooled magnetically stirred solution of 2.15 equivalents of NaOH in 260 ml of H_2O was saturated with H_2S. While H_2S was continued to be introduced into the solution one equivalent of 3-chloro-3-methylbutanone-2 was added dropwise. The addition funnel was washed with 5 ml of methanol. The solution was then stirred for 2 hours at low temperature without H_2S being introduced. Using diluted H_2SO_4 the pH of the solution was adjusted to four. The system was extracted twice using each time 70 ml of CH_2Cl_2. The combined CH_2Cl_2 phase was washed with saturated $NaHCO_3$, washed with water, and dried over Na_2SO_4. The drying agent was removed by filtration and the CH_2Cl_2 was destilled off at normal pressure. ^{1}H NMR spectroscopy of the remaining colorless liquid indicated that less than 5 % impurities were present. Dichloromethane and 3-methylbutanone-2 accounted for most of the impurities. The substance was destilled prior to use (T_b = 100 °C / p = ~20 Torr). Typically, the reaction gave a reproducible isolated yield of m = 36 g / 85 %. The ^{1}H NMR spectrum ($CDCl_3$) of 3-mercapto-3-methylbutanone-2 (**6**) contains three peaks: 1.517 ppm

[$CH_3COCSH(CH_3)_2$], 2.040 ppm [$CH_3COCSH(CH_3)_2$], and 2.326 ppm [$CH_3COCSH(CH_3)_2$].

Synthesis of [Fe(III)pr_2imine$_2Me_2$]PF_6 (**1**):

The purification of this substance proved to be an extreme challenge. A gray powder with an absorption maximum at around 210 nm but no other features possesses very similar solubility properties as the desired product. It was found that the desired product could only be separated from this impurity by mechanical means as described below. The exact identity of this impurity is not known. It is speculated that this gray powder is an 'iron sulfide containing' compound since it gives rise to an absorption in Mössbauer spectroscopy. Earlier Mössbauer measurements of an unclean sample of **1** indicated the presence of three iron-containing impurities: 0.86/3.39, 0.47/1.32, and 0.65/1.96 ($\delta/\Delta E_Q$ in mm/s). Those impurities are not pyrite whose Mössbauer parameters[53] are δ = 0.314 mm/s and ΔE_Q = 0.614 mm/s. The following procedure, provided that the purification is successful, yields reasonable clean compound. All steps were performed in a glove box. In a 50 ml sidearm flask 400 mg NaOH (10 mmol) were dissolved in 10 ml of MeOH under stirring. The 3-mercapto-3-methylbutanone-2 (**6**) (1.182 g, 10 mmol) was added dropwise employing 3 ml of MeOH. This solution was stirred for 30 minutes. In an 100 ml sidearm flask 634 mg (5 mmol) $FeCl_2$ were dissolved in 10 ml of MeOH. The sodiumthiolate solution was then added dropwise to the stirring $FeCl_2$ solution. Initially, the solution is green-brown, after approximately two thirds of the sodiumthiolate solution was added, suddenly, an orange solid began to precipitate. After 20 minutes stirring 656 mg (5 mmol) N-(3-aminopropyl)-1,3-propanediamine were added dropwise employing 3 ml of MeOH. After

10 minutes stirring the solution turned green-brown. After stirring over-night at room temperature, 1.820 g (5.5 mmol) $Fecp_2PF_6$ were added as a solid to the stirring solution. The balance boat and funnel were washed with 10 ml of MeCN. The solution was stirred for 10 minutes at room temperature. The flask with the reaction mixture was then stored at - 35 °C for 4 hours. The reaction mixture was then filtered through celite (wet with MeCN) on a C-frit into a 200 ml flask without washing. Once the solvent was evaporated off, the solid was washed several times with Et_2O until the Et_2O remained nearly colorless. This removed most of the $Fecp_2$. The solid was then dissolved in 15 ml of MeCN. To this stirring solution 7.5 ml of Et_2O were added dropwise. This mixture was filtered after 5 minutes stirring through celite (wet with 50/50 MeCN/Et_2O) on a C-frit into an 100 ml flask. By doing this a brown impurity was separated from the desired product. This step can be repeated using 15 ml of MeCN and 10 ml of Et_2O to ensure that all of this impurity has been separated. After all solvent is evaporated off, the solid was dissolved in 7 ml of MeCN and overlayered with 18 ml of Et_2O. After two days at - 35 °C the mother liquid was decanted while the flask was still cold. The black crystals that remained in the flask where washed several times with Et_2O in the following way. All of the solid in the flask was suspended in Et_2O. Since the black crystals have a higher density they sink to the ground of the flask. In the Et_2O layer a gray solid will remain suspended. Using a pipette the Et_2O containing the suspended gray solid can be separated from the desired product. This mechanical separation is the crucial step in the purification process. The black crystals are then poured into another flask and the last recrystallization and the Et_2O suspension purification are repeated to increase the purity of the

product. By following this procedure, **1** can be obtained (250 mg, 9 % yield) in 95 % purity as estimated by Mössbauer spectroscopy.

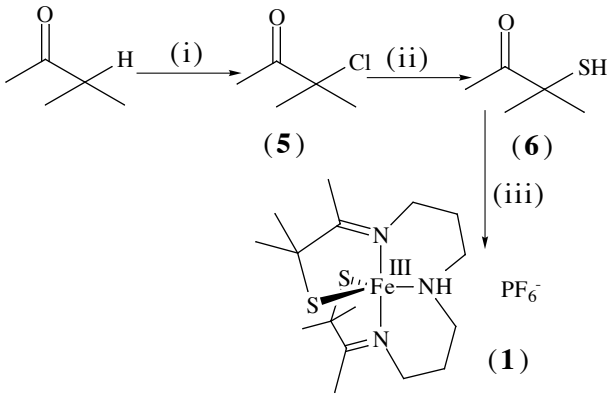


Figure 19. Synthesis of $[Fe(III)pr_2imine_2Me_2]PF_6$ (**1**) [(i) SO_2Cl_2, (ii) NaSH, (iii) $FeCl_2$, $H_2N(CH_2)_3NH(CH_2)_3NH_2$, $Fecp_2PF_6$].

The Mössbauer parameters of **1** are given in table 2 on page 19. They, and the EPR parameters[52] (g_{max} = 2.201, g_{mid} = 2.146, g_{min} = 2.001), are characteristic of low-spin Fe(III). Therefore, **1** is paramagnetic as it is shown in the ^1H NMR spectra in figure 21 and 22. In the range λ = 280 - 600 nm **1** has two absorption maxima which are located at λ_{max} = 316 nm (ε = 6040 l/(mol cm)) and at λ_{max} = 418 nm (ε = 4140 l/(mol cm)). Experiments to assign those bands are in progress at Stanford University.

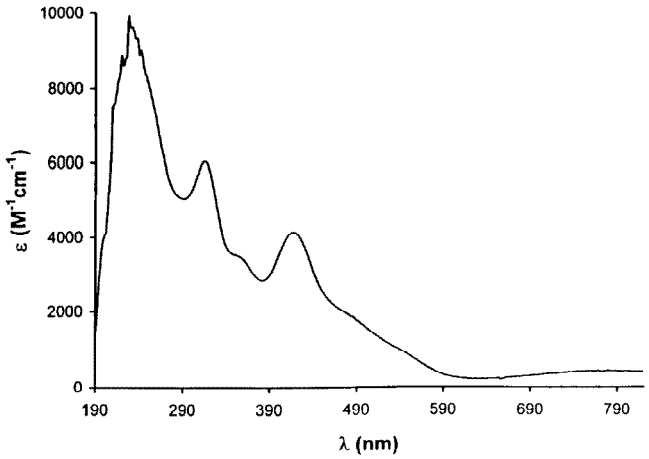


Figure 20. UV/vis Spectrum of $[Fe(III)pr_2imine_2Me_2]PF_6$ (**1**).

The reduction potential of $[Fepr_2imine_2Me_2]^{+/0}$ ($\mathbf{1}^{+/0}$), which is attributed to a change of the iron oxidation state from +3 to +2, is $E_{1/2}$ (Ag^+/Ag) = -714 mV, $E_{1/2}$ (SCE) = -400 mV, $E_{1/2}^-$ = -159 mV, and $E_{1/2}$ (Fc) = -800 mV. To evaluate the influence of the α-methyl groups upon the stability of **1**, one has to compare the reduction potential of **1** with the reduction potential[61] of **3**. The reduction potential of $[Fepr_2imine_2]^{+/0}$ ($\mathbf{3}^{+/0}$), which is attributed to a change of the iron oxidation state from +3 to +2, is $E_{1/2}$ (SCE) = -260 mV, $E_{1/2}^-$ = -19 mV, and $E_{1/2}$ (Fc) = -660 mV. Those results show that the α-methyl groups donate electron density (this is called +I effect) via the sulfurs to the iron. Thus, the equilibrium Fe(III) + e^- = Fe(II) is shifted by 140 mV to the left side in **1** as compared to **3** [Nernst equation: $E = E^- - (RT/\nu F) \ln (a_{right}/a_{left})$, therefore $E^- = (RT/\nu F) \ln (a_{right}/a_{left})$]. In other words, because of the increased electron density at the Fe in **1** it becomes more difficult to add another electron to Fe(III). One can say that the Fe(III) in **1** is stabilized by the presence of the α-methyl groups. Note, that the more negative the reduction potential the more the equilibrium Fe(III) + e^- = Fe(II) is shifted to the left side (Fe(II) becomes a stronger reducing agent and Fe(III) becomes a weaker oxidizing agent).

In summary, it can be said that the α-methyl groups provide two mechanisms to stabilize **1** as compared to **3**. Firstly, they provide a steric protection against oxidation by O_2 at the S and against disulfide formation. Secondly, they donate electron density to the Fe. Thereby, they cause an electronic stabilization of the +3 oxidation state of Fe.

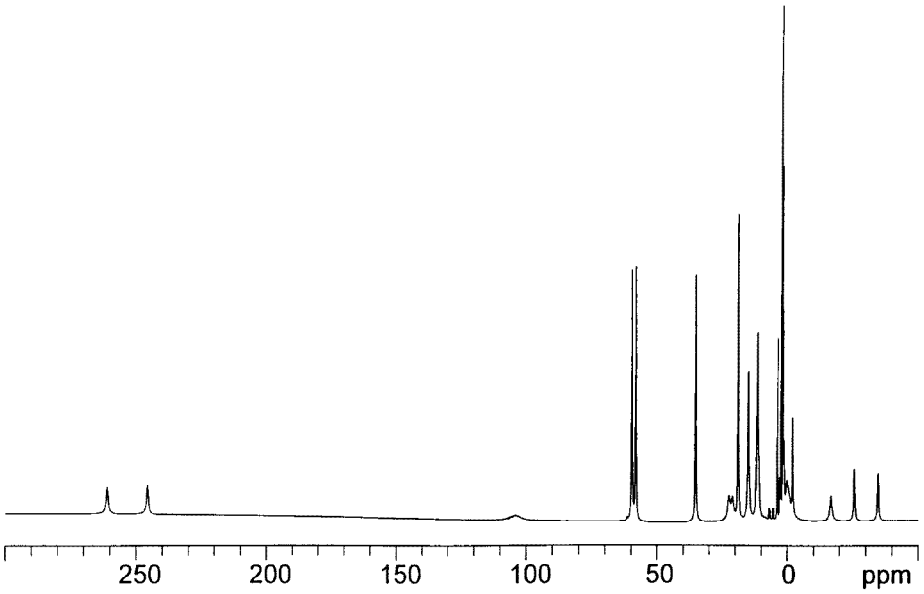


Figure 21. ^{1}H NMR Spectrum of $[Fe(III)pr_2imine_2Me_2]PF_6$ (**1**).

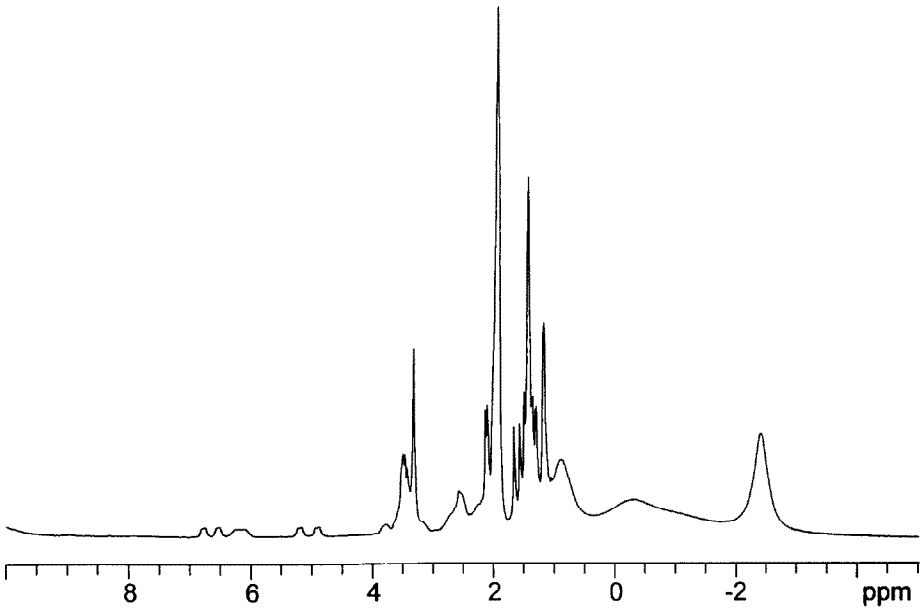


Figure 22. Details of ^{1}H NMR Spectrum of $[Fe(III)pr_2imine_2Me_2]PF_6$ (**1**).

Synthesis of [Fe(III)pr_2imine$_2$$Me_2$(NO)]$PF_6$ (**2**):

Approximately 75 mg of [Fe(III)pr_2imine$_2$$Me_2$]$PF_6$ (**1**) were dissolved in 10 ml of MeCN to give a red solution. On a high vacuum line using a constant volume bulb 1.15 equivalents of NO were added. The NO was allowed to condense in the liquid nitrogen cooled reaction vessel for one hour. After this the reaction vessel was allowed to warm to room temperature under stirring. The reaction system was then taken into a glove box. There the green-brown solution was poured into an 100 ml flask that did not contain a magnetic stirring bar. The solution was overlayered with 90 ml of Et_2O and stored at - 35 °C for 2 days. The mother liquid was decanted off and the remaining black crystals were washed with Et_2O several times. The solid was dried by applying high vacuum for 20 minutes. The crystals obtained in this way were of x-ray quality. Before some of the solid was dissolved in D_6-MeCN to prepare a NMR sample, the solid was dried for an additional 40 minutes under high vacuum. To measure the extinction coefficients the reaction was performed in a vessel to which an UV/vis cell was attached. **2** is stable as a solid in the dark under nitrogen at - 35 °C for weeks.

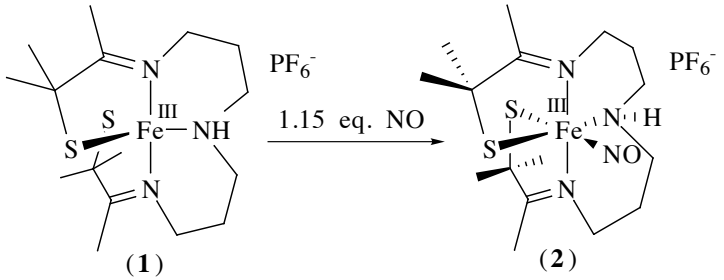


Figure 23. Synthesis of [Fe(III)pr_2imine$_2$$Me_2$(NO)]$PF_6$ (**2**).

[Fe(III)pr_2imine$_2$$Me_2$(NO)]$PF_6$ (**2**) is diamagnetic as proven by ^{1}H NMR, for details see figures 24 and 25. If the NMR is taken using a wider window, see figure 24, also signals corresponding to the paramagnetic **1** can be detected.

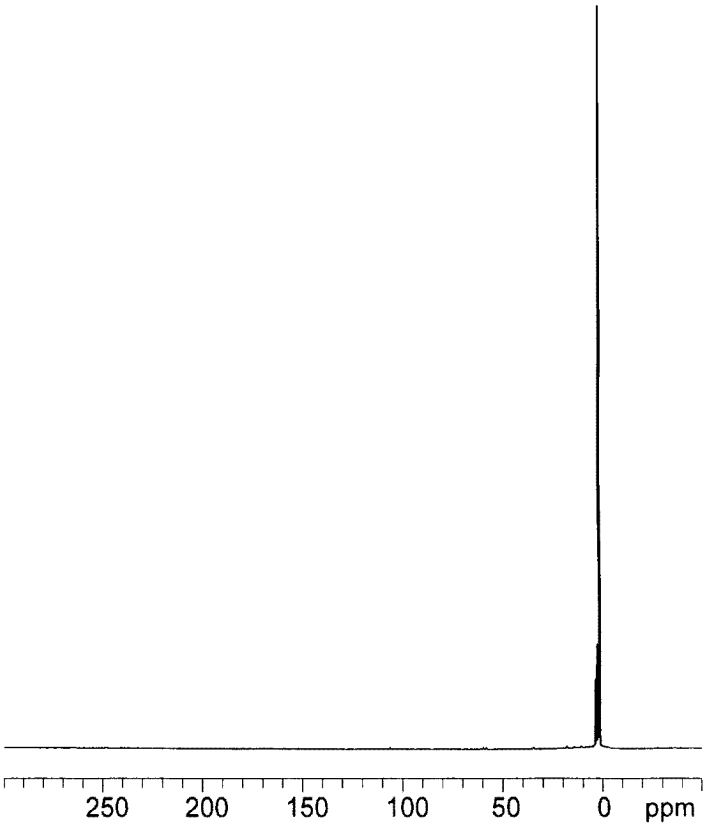


Figure 24. ^{1}H NMR Spectrum of [Fe(III)pr_2imine$_2$$Me_2$(NO)]$PF_6$ (**2**).

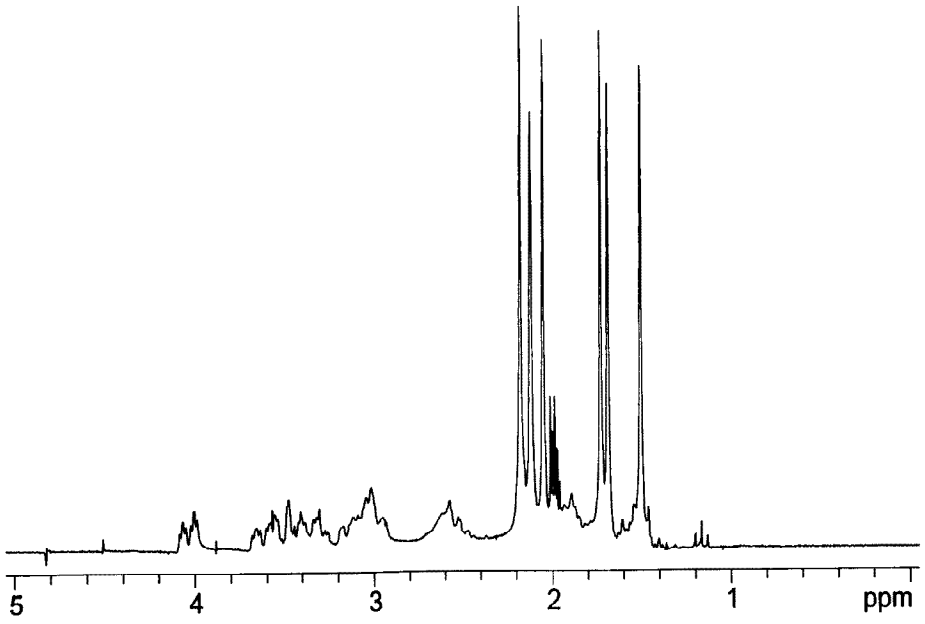


Figure 25. Details of the ^1H NMR Spectrum of $[Fe(III)pr_2imine_2Me_2(NO)]PF_6$ (**2**).

The Mössbauer parameters and EXAFS parameters of **2** are given in table 4 and 5, respectively. In the range λ = 320 - 820 nm **2** has one absorption maximum which is located at λ_{max} = 422 nm (ε = 1710 l/(mol cm)), for details see figure 11 on page 25. IR spectroscopy of **2** showed the νNO to be at 1820 cm^{-1} and the νC=N to be at 1610 cm^{-1}, see figure 26 for details. The crystal structure of **2** was solved in the space group $P2_1/n$ (No. 14) (R = 5.68 %). Since **2** is of c_1 symmetry both enantiomers are present. They are related by an inversion center. When the structure was refined using an Fe-O-N arrangement the R factor was about 5 units higher. Therefore, it was decided that the NO is coordinated to the Fe via its N as opposed to via its O. The ORTEP and selected structural parameters of **2** are shown in figure 10 (see page 25) and table 6 (see page 24), respectively.

The reduction potential of $[Fepr_2imine_2Me_2NO]^{+/0}$ (**2**$^{+/0}$), which is attributed to a change of the iron oxidation state from +3 to +2, is $E_{1/2}$ (Ag^+/Ag) = -769 mV, $E_{1/2}$ (SCE) = -455 mV, $E_{1/2}^-$ = -214 mV, and $E_{1/2}$ (Fc) = -855 mV. From these reduction potentials one can conclude that the Fe(III) in **2** is stabilized by 55 mV as compared to the Fe(III) in **1**.

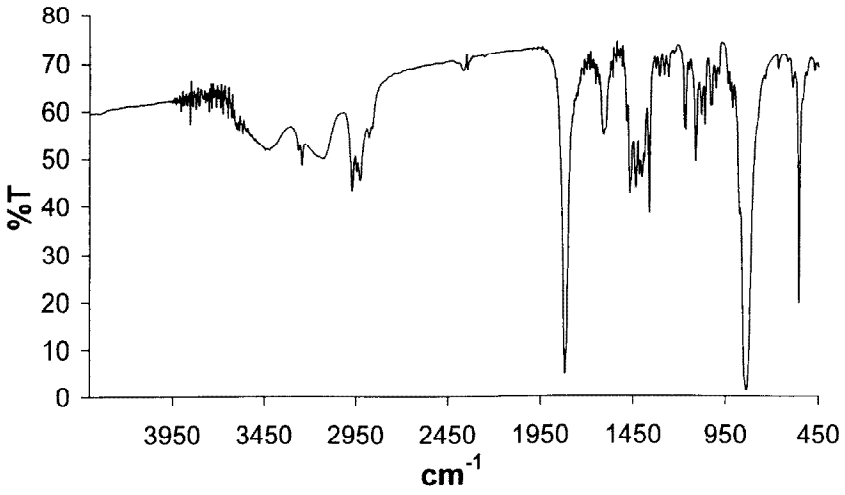


Figure 26. IR Spectrum of $[Fe(III)pr_2imine_2Me_2(NO)]PF_6$ (**2**).

9.) Further Work:

9.1.) Thioimidate Binding to $[Fe(III)pr_2imine_2Me_2]^+$:

Since it is proposed that a thioimidate intermediate (**D**) is part of the catalytic cycle of the hydration of nitrile to form amides by NHase, see figure 6 on page 17, it deems to be reasonable to investigate model compounds of this intermediate. The thioimidate salt shown in figure 27 can be synthesized.[65] It can be deprotonated by triethylamine.[66] This should be done in the presence of $[Fe(III)pr_2imine_2Me_2]^+PF_6^-$ (**1**). The goal would be to isolate a complex that contains the thioimidate bound to $[Fe(III)pr_2imine_2Me_2]^+$ in a fashion that resembles intermediate

D. The spectral properties (UV/vis, IR, NMR, Mössbauer, EPR, Resonance Raman) of this complex can then be studied. Further studies on the enzyme should then be performed. Maybe it is possible to observe a short-lived intermediate with spectral properties resembling those of the thioimidate bound model complex. This would provide further support for the proposed mechanism of nitrile hydration.

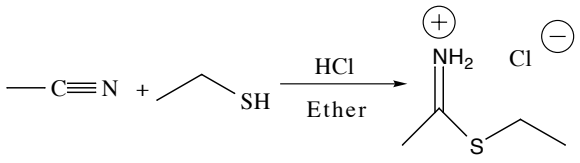


Figure 27. Synthesis of Protonated Thioimidate.

9.2.) Reactivity Model of Nitrile Hydratase:

One of the ultimate aims of this research is, of course, to obtain a small compound that can enantioselectively hydrate nitriles to form amides. The author of this paper believes that compound **7** (see figure 28) or its analogue in which the imines have been reduced, should be able to hydrate nitriles to amides. This compound combines all features known to accelerate the reaction of nitriles with water to form amides. Those features are a metal ion with a +3 charge and a thiol group. The metal ion, in **7** it could be either Fe or Co, serves as a Lewis acid to activate the nitrile.[13] There are a number of enzymes known (see the discussion in chapter 3) in which the thiol group of cysteine attacks a nitrile.

To synthesize **7** a thioamine is necessary. This thioamine is principally accessible according to the two routes shown in figure 28. It has been demonstrated that ethylene oxide in the presence of sulfuric acid will add to the secondary amine of diethylenetriamine to form an

aminoalcohol.[67] Under similar conditions propylene oxide, or propylene sulfide, should react with dipropylenetriamine. The conversion of an OH group to a SH group is known.[68]

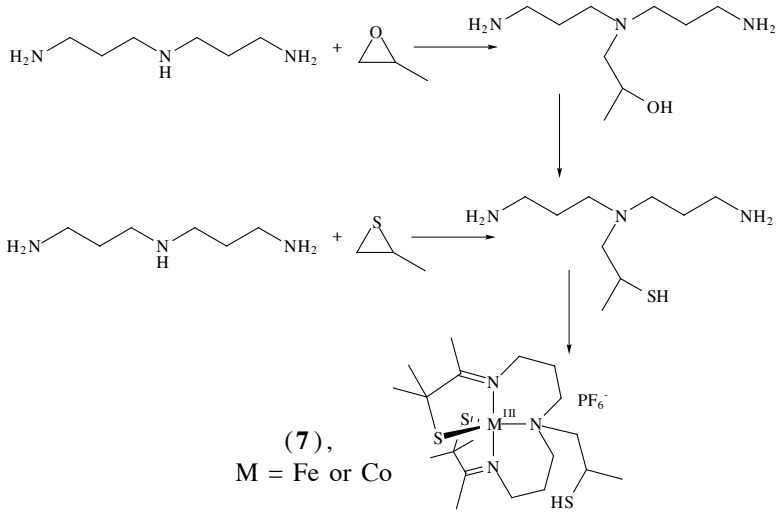


Figure 28. Synthesis of Proposed Reactivity Model of NHase.

9.3.) Structural Models of NHase - Based upon Tc-Chemistry Ligands:

It was discussed above that in the crystal structure of NHase a $N_2S_3O_1$ coordination environment of the Fe center was observed. In radiology, compounds having two amide nitrogens and two thiol sulfurs available for coordination to a metal center are widely used. One could form the Fe complex of such ligands and react it with R-SH, see figure 29 and 30. By doing so, one would expect to obtain a structural model of the crystallographically observed coordination environment of the active site Fe in NHase.

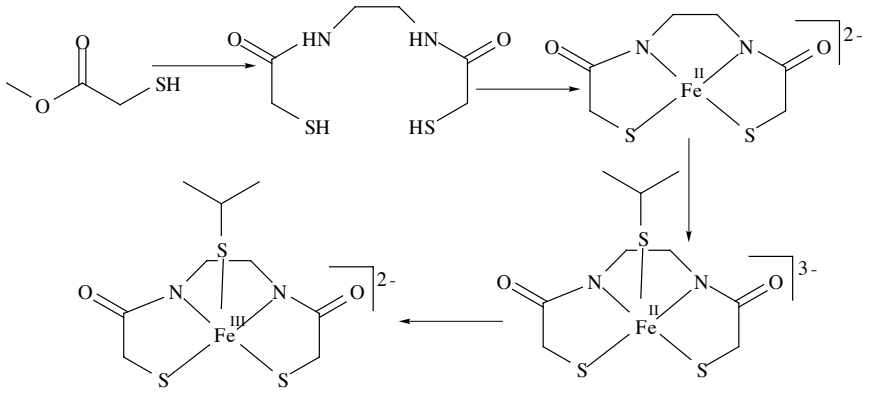


Figure 29. Synthesis of a Structural Model of the Active Site of NHase as Observed by X-ray Crystallography.

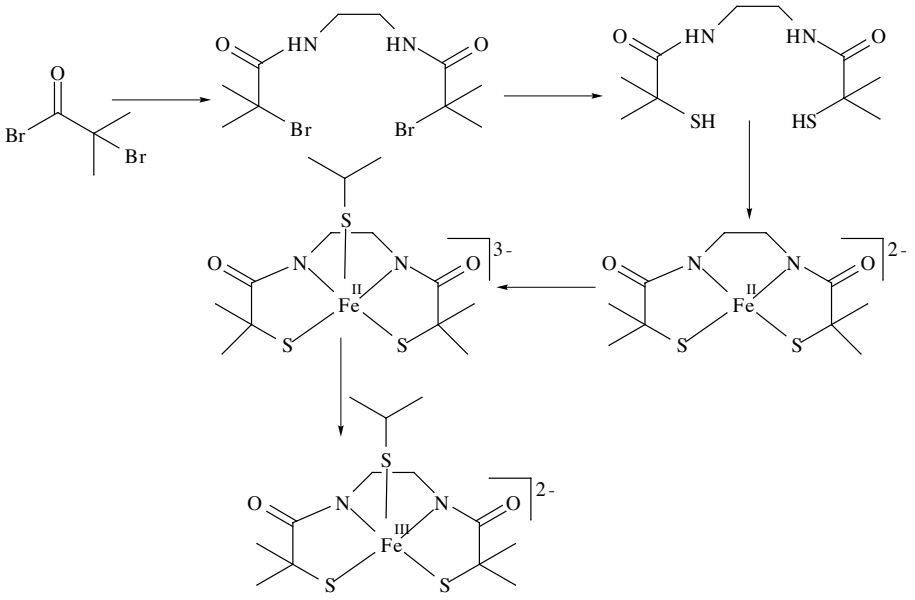


Figure 30. Synthesis of Another Structural Model of the Active Site of NHase as Observed by X-ray Crystallography.

9.4.) A Structural Model of the Crystallographically Observed Coordination Environment of the Active Site Fe in NHase:

It is proposed that the compound (**14**) shown in figure 31 is to be synthesized. This compound provides a close resemblance of the active

site metal coordination environment ($N_2S_3O_1$) found by x-ray crystallography in NHase. Further, the structural model **14** has the advantage over the structural models shown in figures 29 and 30 that each sulfur has two α-methyl groups which will provide steric protection of the sulfur and electronic stabilization of Fe(III) as discussed in chapter 8. The absorption of visible light, the magnetic data, the EPR spectra, and the Mössbauer absorption of this compound should show considerable similarity to the corresponding data of the enzyme. This should help to determine if the coordination environment proposed in the crystal structure is indeed correct. The synthetic route shown in figure 31 should provide access to **14**. All involved reactions are known. It might be necessary to protect the OH group of the bisamine (**10**).

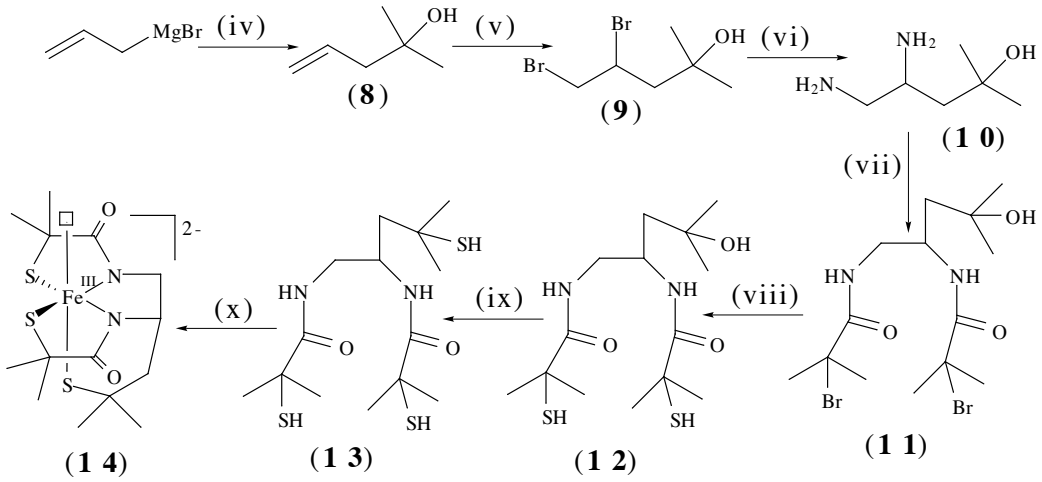


Figure 31. Synthesis of an Exact Structural Model (**14**) of the Active Site of NHase as Observed by X-ray Crystallography [(iv) $(CH_3)_2CO$, H_2O, (v) Br_2, (vi) aq. NH_3, (vii) $BrCOC(CH_3)_2Br$, pyridine, (viii) NaSH, (ix) AcSH, Diisopropylazodicarboxylate, PPh_3, THF, $NaOH/H_2O$ (x) NaOH, $FeCl_2$, $Fecp_2PF_6$].

9.5.) Other Ideas:

As it was discussed in chapter 6, one should, in addition to **2**, synthesize an $\{FeNO\}^6$ model compound having a $N_2S_3(NO)$ coordination environment. One should then compare the spectral parameters of this model compound and of **2** with the spectral parameters of NO-inactivated NHase. This would further help to assign a correct coordination environment to the active site Fe in NO-inactivated NHase.

It was mentioned in the introduction that two other enzymes having an Fe ion in a mixed N/O/S coordination environment are known. Those enzymes are desulfoferrodoxin (center II) and neelaredoxin. They contain high-spin Fe(III) in a $N_4S_1O_1$ coordination environment. The nitrogens are imidazole nitrogens of histidine. The open coordination site and the coordinating sulfur, which is derived from cysteine, are *trans* to each other. Even through their active center does not contain low-spin Fe(III), it is interesting to model their active center. So far, no function of desulfoferrodoxin and neelaredoxin is known. Maybe the study of a structural and spectroscopic model compound of their active center will enable scientists to recognize a potential function of desulfoferrodoxin and neelaredoxin.

10.) Conclusions:

The research described in the preceding chapters clearly shows that it is possible to model the spectroscopic and structural properties of active NHase, NO-inactivated NHase, and the short-lived NHase intermediate. Efforts to model the catalytic properties of NHase are underway.

Especially exciting is the successful modeling of the spectroscopic, and therefore most likely also structural, properties of the short-lived NHase intermediate. This means, it is possible to synthesize a small molecule which resembles an enzyme intermediate!

The further study of the above mentioned compounds and the compounds proposed in chapter 9 will enable one to determine on a molecular level which structural and electronic properties are responsible for tuning the catalytic reactivity of NHase just right, so that only one reaction is catalyzed. This one reaction has to be catalyzed with the highest possible rate, but with the lowest possible amount of side products.

The basic strategy of the herein described research applies equally well to the study of any other metalloenzyme. The study of small compounds will enable bioinorganic chemists to understand the structure - function relationship of enzymes, as well as how the catalytic reactivity of an enzyme is regulated. This provides the prospect to understand nature, and, it will enable scientists to develop novel catalysts. Those novel catalysts will be small molecules which enantioselectively catalyze only one reaction. This will enable humankind to synthesize needed compounds in a much more efficient way than it is done today.

11.) References:

1) PROMISE - The Prosthetic Groups and Metal Ions in Protein Active Sites Database, Version 1.5; March **1998**; (http://bmbsgi11.leeds.ac.uk/promise/).

2) Coelho, A. V., Matias, P., Fülöp, V., Thompson, A., Gonzalez, A., and Carrondo, M. A.; Desulfoferrodoxin Structure Determined by MAD Phasing and Refinement to 1.9 Å Resolution Reveals a Unique Combination of a Tetrahedral FeS_4 Centre with a Square Pyramidal $FeSN_4$ Centre; *Journal of Biological Inorganic Chemistry*, **1997**, 2, 680-689.

3) Chen, L., Sharma, P., Le Gall J., Mariano, A. M., Teixeira, M., and Xavier, A. V.; A Blue Non-heme Iron Protein from *Desulfovibrio gigas*; *European Journal of Biochemistry*, **1994**, 226, 613-618.

4) Münck, E., Nelson, M., Huynh, B. H., Kovacs, J. A., and Schweitzer, Dirk; Manuscript in Preparation.

5) Ellison, J. J., Schweitzer, D., Shoner, S. C., Lovell, S., and Kovacs, J. A.; A Synthetic Model for the NO-Inactivated Form of Nitrile Hydratase; *Journal of the American Chemical Society*, Submitted for Publication.

6) Brennan, B. A., Alms, G., Nelson, M. J., Durney, L. T., and Scarrow, R. C.; Nitrile Hydratase from *Rhodococcus rhodochrous* J1 Contains an Non-Corrin Cobalt Ion with Two Sulfur Ligands; *Journal of the American Chemical Society*, **1996**, 118, 9194-9195.

7) Peters, J. W., Stowell, M. H. B., Soltis, S. M., Finnegan, M. G., Johnson, M. K., and Rees, D. C.; Redox-Dependent Structural Changes in the Nitrogenase P-Cluster; *Biochemistry*, **1997**, 36, 1181-1187.

8) Yamada, H. and Kobayashi, M.; Nitrile Hydratase and Its Application to Industrial Production of Acrylamide; *Bioscience, Biotechnology, and Biochemistry*, **1996**, 60, 1391-1400.

9) Wyatt, J. M. and Knowles, C. J.; Microbial Degradation of Acrylonitrile Waste Effluents: the Degradation of Effluents and Condensates from the Manufacture of Acrylonitrile; *International Biodeterioration & Biodegradation*, **1995**, 35, 227-248.

10) Kobayashi, M., Komeda, H., Yanaka, N., Nagasawa, T., and Yamada, H.; Nitrilase from *Rhodococcus rhodochrous* J1; *The Journal of Biological Chemistry*, **1992**, 267, 20746-20751.

11) Baker, R. T. and Varshavsky, A.; Yeast N-terminal Amidase; *The Journal of Biological Chemistry*, **1995**, 270, 12065-12074.

12) Lee, Y. B., Goo, Y. M., Lee, Y. Y., and Lee, J. K.; Hydrolysis of Various Nitrile Compounds to the Amides by Catalysis of 2-Mercaptoethanol in a Phosphate Buffer; *Tetrahedron Letters*, **1989**, 30, 7439-7440.

13) Buckingham, D. A., Keene, F. R., and Sargeson, A. M.; Base Hydrolysis of Coordinated Acetonitrile; *Journal of the American Chemical Society*, **1973**, 95, 5649-5652.
Herein acetonitrile was coordinated to $Co(NH_3)_5^{3+}$.

14) Odaka, M., Noguchi, T., Nagashima, S., Yohda, M., Yabuki, S., Hoshino, M., Inoue, Y., and Endo, I.; Location of the Non-Heme Iron Center on the α Subunit of Photoreactive Nitrile Hydratase from *Rhodococcus* sp. N-771; *Biochemical and Biophysical Research Communications*, **1996**, 221, 146-150.

15) a) Nelson, M. J., Jin, H., Turner, I. M., Jr., Grove, G., Scarrow, R. C., Brennan, B. A., and Que, L., Jr.; A Novel Iron-Sulfur Center in Nirile Hydratase from *Brevibacterium* sp.; *Journal of the American Chemical Society*, **1991**, 113, 7072-7073.

b) Payne, M. S., Wu, S., Fallon, R. D., Tudor, G., Stieglitz, B., Turner, I. M., Jr., and Nelson, M. J.; A Stereoselective Cobalt-Containing Nitrile Hydratase; *Biochemistry*, **1997**, 36, 5447-5454.

c) Fallon, R. D., Stieglitz, B., and Turner, I., Jr.; A *Pseudomonas putida* Capable of Stereoselective Hydrolysis of Niriles; *Applied Microbiology and Biotechnology*, **1997**, 47, 156-161.

d) Bauer, R., Knackmuss, H.-J., and Stolz, A.; Enantioselective Hydration of 2-arylpropionitriles by a Nitrile Hydratase from *Agrobacterium tumefaciens* Strain d3; *Applied Microbiology and Biotechnology*, **1998**, 49, 89-95.

16) Huang, W., Jia, J., Cummings, J., Nelson, M., Schneider, G., and Lindqvist, Y.; Crystal Structure of Nitrile Hydratase Reveals a Novel Iron Centre in a Novel Fold; *Structure*, **1997**, 5, 691-699.

17) Sugiura, Y., Kuwahara, J., Nagasawa, T., and Yamada, H.; Nitrile Hydratase: The First Non-Heme Iron Enzyme with a Typical Low-Spin Fe(III)-Active Center; *Journal of the American Chemical Society*, **1987**, 109, 5848-5850.

18) a) Kaim, W. and Schwederski, B.; Bioanorganische Chemie; Teubner, **1991**.

b) Lippard, S. J. and Berg, J. M.; Principles of Bioinorganic Chemistry; University Science Books, **1994**.

19) Kobayashi, M., Suzuki, T., Fujita, T., Masuda, M., and Shimizu, S.; Occurrence of Enzymes Involved in Biosynthesis of Indole-3-Acetic Acid from Indole-3-Acetonitrile in Plant-Associated Bacteria, *Agrobacterium* and *Rhizobium*; *Proceedings of the National Academy of Science of the United States of America*, **1995**, 92, 714-718.

20) Boehlein, S. K., Rosa-Rodriguez, J. G., Schuster, S. M., and Richards, N. G. J.; Catalytic Activity of the N-Terminal Domain of *Escherichia coli* Asparagine Synthetase B Can Be Reengineered by Single-Point Mutation; *Journal of the American Chemical Society*, **1997**, 119, 5785-5791.

21) Noveron, J. C., Olmstead, M. M., and Mascharak, P. K.; Effect of Carboxamido N Coordination to Iron on the Redox Potential of Low-Spin Non-Heme Iron Centers with N,S Coordination: Relevance to the Iron Site of Nitrile Hydratase; *Inorganic Chemistry*, **1998**, 37, 1138-1139.

22) Nagasawa, T., Ryuno, K., and Yamada, H.; Nitrile Hydratase of *Brevibacterium* R312; *Biochemical and Biophysical Research Communications*, **1986**, 139, 1305-1312.

23) It is known that some fungi express cyanide hydratase, which has sequence homology to nitrilase, to remove toxic cyanide. In some cases organisms might be expressing NHase to remove potentially toxic nitriles. It might also be that cyanide is first enzymatically methylated and then degradated by NHase. However, no enzyme having the activity to methylate cyanide is known to the author of this paper. Wang, P. and VanEtten, H. D.; Cloning and Properties of a Cyanide Hydratase Gene from the Phytopathogenic Fungus *Gloeocercospora sorghi*; *Biochemical and Biophysical Research Communications*, **1992**, 187, 1048-1054.

24) Nagasawa, T. and Yamada, H.; Microbial Transformations of Nitriles; *Trends in Biotechnology*, **1989**, 7, 153-158.

25) Meth-Cohn, O. and Wang, M.-X.; An In-Depth Study of the Biotransformation of Nitriles into Amides and/or Acids Using *Rhodococcus rhodochrous* AJ270; *Journal of the Chemical Society, Perkin Transactions I*, **1997**, 1099-1104.

26) a) Shoner, S. C., Barnhart, D., and Kovacs, J. A.; A Model for the Low-Spin, Non-Heme, Thiolate-Ligated Iron Site of Nitrile Hydratase; *Inorganic Chemistry*, **1995**, 34, 4517-4518.

b) Jackson, H. L. and Kovacs, J. A.; Manuscript in Preparation.

c) Nivorozhkin, A. L., Uraev, A. I., Bondarenko, G. I., Antsyshkina, A. S., Kurbatov, V. P., Garnovskii, A. D., Turta, C. I., Brashoveanu, N. D.; Iron Complexes with an N/S Chromophore Relevant to the Active Site of the Hydrolytic Metalloenzyme Nitrile Hydratase; *Chemical Communications*, **1997**, 1711-1712.

27) Dr. Weijun Huang; Personal Communication; October **1997**.

28) Nagamune, T., Kurata, H., Hirata, M., Honda, J., Koike, H., Ikeuchi, M., Inoue, Y., Hirata, A., and Endo, I.; Purification of Inactivated Photoresponsive Nitrile Hydratase; *Biochemical and Biophysical Research Communications*, **1990**, 168, 437-442.

29) The concept of this figure was developed by Dr. J. J. Ellison.

30) Noguchi, T., Honda, J., Nagamune, T., Sasabe, H., Inoue, Y., and Endo, I.; Photosensitive Nitrile Hydratase Intrinsically Possesses Nitric Oxide Bound to the Non-Heme Iron Center: Evidence by Fourier Transform Infrared Spectroscopy; *FEBS Letters*, **1995**, 358, 9-12.

31) Odaka, M., Fujii, K., Hoshino, M., Noguchi, T., Tsujimura, M., Nagashima, S., Yohda, M., Nagamune, T., Inoue, Y., and Endo, I.; Activity Regulation of Photoreactive Nitrile Hydratase by Nitric Oxide; *Journal of the American Chemical Society*, **1997**, 119, 3785-3791.

32) Noguchi, T., Hoshino, M., Tsujimura, M., Odaka, M., Inoue, Y., and Endo, I.; Resonance Raman Evidence that Photodissociation of Nitric Oxide from the Non-Heme Iron Center Activates Nitrile Hydratase from *Rhodococcus* sp. N-771; *Biochemistry*, **1996**, 35, 16777-16781.

33) Bonnet, D., Artaud, I., Moali, C., Pétré, D., and Mansuy, D.; Highly Efficient Control of Iron-Containing Nitrile Hydratases by Stoichiometric Amounts of Nitric Oxide and Light; *FEBS Letters*, **1997**, 409, 216-220.

34) It is unclear to the author of this paper how the difference in the Mössbauer data of the active form of NHase from reference 4 and from this reference can be explained. The value of the quadrupole splitting constant (ΔE_Q = 0.37 mm/s) obtained by the researchers in Japan is typical[26c] for four-coordinated high-spin (S = 5/2) Fe(III) complexes having a very symmetrical electron environment (*e.g.* $FeCl_4^-$). It might be that the data shown in reference 34 was obtained from a sample containing NO-inactivated NHase and $FeCl_4^-$.

a) Honda, J., Teratani, Y., Kobayashi, Y., Nagamune, T., Sasabe, H., Hirata, A., Ambe, F., and Endo, I.; Light-Induced Oxidation of Iron Atoms in a Photosensitive Nitrile Hydratase; *FEBS Letters*, **1992**, 301, 177-180.

b) Nagamune, T., Honda, J., Kobayashi, Y., Sasabe, H., Endo, I., Ambe, F., Teratani, Y., and Hirata A.; Mössbauer, Electron Paramagnetic Resonance and Magnetic Susceptibility Studies of Photosensitive Nitrile Hydratase from *Rhodococcus* sp. N-771; *Hyperfine Interactions*, **1992**, 71, 1271-1274.

35) Dufour, E., Storer, A. C. and Ménard, R.; Engineering Nitrile Hydratase Activity into a Cysteine Protease by a Single Mutation; *Biochemistry*, **1995**, 34, 16382-16388.

36) Kopf, M.-A., Bonnet, D., Artaud, I., Pétré, D., and Mansuy, D.; Key Role of Alkanoic Acids on the Spectral Properties, Activity, and Active-Site Stability of Iron-Containing Nitrile Hydratase from *Brevibacterium* R312; *European Journal of Biochemistry*, **1996**, 240, 239-244.

37) Ellison, J. J., Nienstedt, A. M., Shoner, S. C., Barnhart, D., Cowen, J. A., and Kovacs, J. A.; Reactivity of Five-Coordinated Models for the Thiolate-Ligated Fe Site of Nitrile Hydratase; *Journal of the American Chemical Society*, In Press.
Herein the binding of azide to compound **1** was investigated.

38) Miessler, G. L. and Tarr, D. A.; Inorganic Chemistry; Prentice Hall, **1991**.

39) Jin, H., Turner, I. M., Jr., Nelson, M. J., Gurbiel, R. J., Doan, P. E., and Hoffman, B. M.; Coordination Sphere of the Ferric Ion in Nitrile Hydratase; *Journal of the American Chemical Society*, **1993**, 115, 5290-5291.

40) Brennan, B. A., Cummings, J. G., Chase, B., Turner, I. M., Jr., and Nelson, M. J.; Resonance Raman Spectroscopy of Nitrile Hydratase, a Novel Iron-Sulfur Enzyme; *Biochemistry*, **1996**, 35, 10068-10077.

41) Scarrow, R. C., Brennan, B. A., Cummings, J. G., Jin, H., Duong, D. J., Kindt, J. T., and Nelson, M. J.; X-ray Spectroscopy of Nitrile Hydratase at pH 7 and 9; *Biochemistry*, **1996**, 35, 10078-10088.

42) A search of the Cambridge Structure Database in March of **1998** showed the Fe-NO distance to be 1.671 ± 0.057 Å and the FeN-O distance to be 1.166 ± 0.034 Å. In this analysis only terminal FeNO were considered and all Fe oxidation states were included.[58] When this search was limited to $\{FeNO\}^6$ systems, 13 structures were found. Their Fe-NO bond lengths ranged from 1.62 - 1.68 Å, and their mean N-O distance was 1.143 Å.[46]

43) Scarrow, R. C., Strickler, B. S., Ellison, J. J., Shoner, S. C., Kovacs, J. A., Cummings, J. G., and Nelson, M. J.; X-ray Spectroscopy of Nitric Oxide Binding to Iron in Inactive Nitrile Hydratase and a Synthetic Model Compound; *Journal of the American Chemical Society*, Submitted for Publication.

44) Tsujimura, M., Dohmae, N., Odaka, M., Chijimatsu, M., Takio, K., Yohda, M., Hoshino, M., Nagashima, S., and Endo, I.; Structure of the Photoreactive Iron Center of the Nitrile Hydratase from *Rhodococcus* sp. N-771; *The Journal of Biological Chemistry*, **1997**, 272, 29454-29459.

45) Constable, E. C.; Metals and Ligand Reactivity; VCH, **1996**.

46) Prof. Julie A. Kovacs; Personal Communication.

47) Based upon earlier Mössbauer measurements of compound **1**, it is estimated that the chemical yield is less than 60%.

48) Drago, R. S.; Physical Methods for Chemists; Saunders College Publishing, **1992**.

49) Shoner, S. C., Nienstedt, A. M., Ellison, J. J., Kung, I. Y., Barnhart, D., and Kovacs, J. A.; Structural Comparison of Thiolate-Ligated M^{II}=Fe^{II}, Co^{II}, Ni^{II}, and Zn^{II} Ions Wrapped in a Chiral Helical Ligand; *Inorganic Chemistry*, Submitted for Publication.

50) a) Butler, A. R. and Williams, D. L. H.; The Physiological Role of Nitric Oxide; *Chemical Society Reviews*, **1993**, 233-241.

b) The complete volumes 268 and 269, both **1996**, of *Methods in Enzymology* are dedicated to NO in biological systems.

51) Prof. B. H. (Vincent) Huynh, Unpublished Results.

52) Dr. Mark J. Nelson, Unpublished Results.

53) Greenwood, N. N. and Gibb, T. C.; Mössbauer Spectroscopy; Chapman and Hall Ltd., **1971**.

54) Richter-Addo, G. B. and Legzdins, P.; Metal Nitrosyls; Oxford University Press, **1992**.

55) Enemark, J. H. and Feltham, R. D.; Principles of Structure, Bonding, and Reactivity for Metal Nitrosyl Complexes; *Coordination Chemistry Reviews*, **1974**, 13, 339-406.

56) Chemical Rubber Company Handbook of Chemistry and Physics, CRC Press, **1994**.

57) Sellmann, D., Kunstmann, H., Moll, M., and Knoch, F.,; Transition Metal Complexes with Sulfur Ligands; *Inorganica Chimica Acta*, **1988**, 154, 157-167. For two similar ligand systems reported herein the ν_{NO} of the $\{FeNO\}^7$ complex ('Fe(I) and NO^{+}' , 'Fe(II) and NO•' , 'Fe(III) and NO^{-}') is around 1630 cm^{-1}, while the ν_{NO} of the $\{FeNO\}^6$ complex is around 1870 cm^{-1}.

58) Dirk Schweitzer; Unpublished Results.

59) It was however shown that **1**, when dissolved in MeOH, decomposes with an estimated rate of 15%/24 h in the dark at room temperature. Dirk Schweitzer and Jeff Ellison; Unpublished Results.

60) Connelly, N. G. and Geiger, W. E.; Chemical Redox Agents for Organometallic Chemistry; *Chemical Reviews*, **1996**, 96, 877-910.

61) Dr. Jeff J. Ellison; Unpublished Results.

62) Gritzner, G. and Kuta, J.; Recommendations on Reporting Electrode Potentials in Nonaqueous Solvents; *Pure & Applied Chemistry*, **1984**, 56, 461-466.

63) Wyman, D. P. and Kaufman, P. R.; The Chlorination of Active Hydrogen Compounds with Sulfuryl Chloride. I. Ketones; *Journal of Organic Chemistry*, **1964**, 29, 1956-1960.

64) Asinger, F., Thiel, M., and Esser, G.; Die Herstellung von Thiazolinen-Δ3 durch Gemeinsame Einwirkung von Ammoniak und Oxo-Verbindungen auf α-Mercaptoketone; *Liebigs Annalen der Chemie*, **1957**, 610, 33-49.

65) Schmidt, E.; Über Alkylierte Iso-[acyl-glykokollester] und Phenylhydrazidoester; *Berichte der Deutschen Chemischen Gesellschaft*, **1914**, 47, 2545-2550.

66) Kotyñski, A. and Stec, W. J.; Synthesis of 1-Aminoethylphosphonic Acid; *Polnish Journal of Chemistry*, **1978**, 52, 659-662.
Herein, Et_3N was used to deprotonate Methylthioimidate. Since it can be assumed that the pKa is effectively the same, Et_3N will also be able to deprotonate Ethylthioimidate.

67) Bobylev, V. A. and Chechik, V. O.; Synthesis of N-(2-Hydroxyethyl)- and N-(2-Chloroethyl)-Polyethylenepolyamines; *Journal of General Chemistry of the USSR* (English Translation), **1990**, 60, 2438-2442.

68) Volante, R. P.; A New, Highly Efficient Method for the Conversion of Alcohols to Thiolesters and Thiols; *Tetrahedron Letters*, **1981**, 22, 3119-3122.